DEUTSCHES ELEKTRONEN-SYNCHROTRON DESY

DESY 80/88
September 1980

WEAK NEUTRAL CURRENT EFFECTS IN e^+e^- ANNIHILATION

by

G. Schierholz
II. Institut für Theoretische Physik der Universität Hamburg

D. H. Schiller
Fachbereich Physik, Gesamthochschule Siegen

NOTKESTRASSE 85 · 2 HAMBURG 52

To be sure that your preprints are promptly included in the
HIGH ENERGY PHYSICS INDEX ,
send them to the following address (if possible by air mail) :

DESY
Bibliothek
Notkestrasse 85
2 Hamburg 52
Germany

DESY 80/88
September 1980

WEAK NEUTRAL CURRENT EFFECTS IN e^+e^- ANNIHILATION

by

G. Schierholz
II. Institut für Theoretische Physik der Universität Hamburg

D. H. Schiller
Fachbereich Physik, Gesamthochschule Siegen

Abstract:

We discuss the differential cross sections and angular correlations for $e^+e^- \to \gamma, Z^o \to f\bar{f} \to$ (arbitrary final state) for arbitrarily polarized electron/positron beams (f stands for any lepton or quark). Special application to three-jet final states (including that of two jets) is furnished.

1. Introduction

At higher energies, the annihilation of electron-positron pairs through the neutral intermediate Z^o boson becomes increasingly important. The Z^o has vector and axial vector couplings to leptons and quarks which, interfering with the one-photon exchange diagrams, will manifest itself in a rather different structure of the final state.

There is considerable theoretical interest in determining the weak neutral current couplings of leptons and quarks. For example, the Weinberg-Salam model [1] predicts the neutral couplings to be the same for each family of leptons and quarks, and one would like to test this prediction. Since heavy leptons and quarks will be more abundant in e^+e^- annihilation than elsewhere, this is the ideal laboratory for studying neutral currents. There should be no serious difficulty in identifying the quark quantum numbers, at least not for the heavy quarks.

But also for strong interaction studies (jet physics) the increasing weak neutral current contribution is of great interest. For example, the presence of weak and electromagnetic interferences will bring forth certain observables which, otherwise, require longitudinal beam polarization to be measured. The observables we have in mind [2,3] have the unique feature of giving direct indication of the chromodynamic gluon self-couplings. Near the Z^o pole there is, furthermore, the possibility of detailed studies of multi-jet events with high statistics — in such abundance not available anywhere else.

Despite the many recent contributions to this subject [4-8], a systematic study of the weak neutral current effects in e^+e^- annihilation is lacking. In particular, leptons and quarks have always been considered to be massless, which certainty cannot be maintained for the yet to be descovered top quark, and the hadronic tensor was assumed to be purely real. We have learned, however, that the imaginary part of the hadronic tensor is of great importance for testing QCD [2,3]. It is the aim of this paper to discuss the differential cross sections and angular distributions for an arbitrary final state (multi-jet, semi-inclusive, etc.) and arbitrarity polarized beams. As is well known, one needs longitudinal polarization in order to determine the relative sign of the vector and axial vector couplings while transverse polarization might help to disentangle the various cross sections such as the counter parts of σ_U, σ_L, etc. [9,10].

The organization of the paper is as follows. In section 2 and appendix A and B we discuss the differential cross sections as well as the leptonic and hadronic tensors. In section 3 this is applied to planar events (including two-jet topologies as the limiting case), the most prominent multi-jet events. Finally, in section 4 we give the cross sections for $e^+e^- \to q\bar{q}g$ in tree approximation.*)

*) These have been given before in Ref.[6].

2. Differential cross sections and angular distributions

We consider electron-positron annihilation in the 1γ- and 1Z^o-exchange approximation. The virtual photon γ and the neutral intermediate boson Z^o are supposed to couple to the final state through a spin-1/2 fermion-antifermion pair $f\bar{f}$, which might then transform into an arbitrary final state F (Fig.1).

The electromagnetic and weak (neutral current) couplings are defined by the following Lagrangean densities

$$\mathcal{L}_{e.m.} = -e\left[Q_e \bar{\Psi}_e \gamma^\mu \Psi_e + Q_f \bar{\Psi}_f \gamma^\mu \Psi_f\right] A_\mu ,$$

$$\mathcal{L}_{n.c.} = -eM_Z\sqrt{g}\left[\bar{\Psi}_e \gamma^\mu (v - a\gamma_5)\Psi_e + \bar{\Psi}_f \gamma^\mu (v_f - a_f\gamma_5)\Psi_f\right] Z_\mu , \tag{2.1}$$

where the Dirac fields ψ_e, ψ_f and the vector fields A^μ, Z^μ describe, respectively, the electron e^-, the fermion f, the photon γ and the neutral intermediate boson Z^o of mass M_Z; $Q_e = -1$ and Q_f give the electric charge of e^- and f (in units of $e = \sqrt{4\pi\alpha}$, with $\alpha = 1/137$ the fine structure constant), whereas $v(v_f)$ and $a(a_f)$ determine the strength of the vector and axial-vector couplings of the Z^o at the electron (fermion) vertex in terms of the dimensionless coupling constant $eM_Z\sqrt{g}$, with g related to the Fermi weak coupling constant G_F by $g = G_F(8\sqrt{2}\,\pi\alpha)^{-1} \approx 4.49 \times 10^{-5}$ GeV^{-2}.

The Feynman amplitude for the process $e^-(p_-) + e^+(p_+) \to \gamma, Z(q) \to F$ (final state) has the general structure

$$M_{FI} = eQ_e \bar{v}(p_+)\gamma^\mu u(p_-) \frac{-g_{\mu\nu}}{q^2 + i0} J^\nu_{e.m.}$$

$$+ eM_Z\sqrt{g}\, \bar{v}(p_+)\gamma^\mu(v - a\gamma_5)u(p_-) \frac{-g_{\mu\nu} + q_\mu q_\nu/M_Z^2}{q^2 - M_Z^2 + iM_Z\Gamma_Z}\left(V^\nu_{n.c.} - A^\nu_{n.c.}\right), \tag{2.2}$$

where Γ_Z is the total decay width of the Z^o-boson and $J^\nu_{e.m.}$, $V^\nu_{n.c.}$ and $A^\nu_{n.c.}$ refer, respectively, to the electromagnetic, weak neutral vector and weak neutral axial-vector vertices of the final state, i.e. $J^{\nu}_{e.m.} \sim \langle F|J^{\nu}_{e.m.}(0)|0\rangle$, etc. In the special case of Fig. 1, when the photon and the Z^0-boson couple to the final state via a fermion-antifermion pair with couplings given by (2.1), one simply has

$$J^{\nu}_{e.m.} = e Q_f J^{\nu}_f ,$$

$$V^{\nu}_{n.c.} = e M_Z \sqrt{g}\, v_f J^{\nu}_f ,$$

$$A^{\nu}_{n.c.} = e M_Z \sqrt{g}\, a_f A^{\nu}_f , \tag{2.3}$$

where the same J^{ν}_f appears in $J^{\nu}_{e.m.}$ and in $V^{\nu}_{n.c.}$. Using $q = p_- + p_+$ and the Dirac equation for the leptons, one finds $\bar{v}_+ \not{q} (v - a\gamma_5) u_- = 2m_e a\, \bar{v}_+ \gamma_5 u_-$; thus there is no contribution coming from the term $q^{\mu} q^{\nu}/M_Z^2$ of the Z^0-propagator if the electron mass m_e is neglected. In this case (2.2) reduces to

$$M_{FI} = -\frac{e^2}{s}\Big\{ Q_e Q_f\, \bar{v}(p_+)\gamma_{\mu} u(p_-)\, J^{\mu}_f$$

$$+ \chi_Z(s)\, \bar{v}(p_+)\gamma_{\mu}(v - a\gamma_5) u(p_-) \left(v_f J^{\mu}_f - a_f A^{\mu}_f\right)\Big\} , \tag{2.4}$$

where $s = q^2$ is the total center of mass energy squared and

$$\chi_Z(s) = g M_Z^2 s \left(s - M_Z^2 + i M_Z \Gamma_Z\right)^{-1} . \tag{2.5}$$

The differential cross section for an arbitrary N-particle final state, summed over the final spin orientations and for arbitrary polarized beams is then given by

$$d^{3N}\sigma^f = \left(\frac{2\pi\alpha}{s}\right)^2 \Big[\sum_{r',r=1}^{4} g^f_{r'r}(s)\, L_{r'} \cdot H^f_r \Big]$$

$$\cdot (2\pi)^4 \delta_4\Big(\sum_{n=1}^{N} p_n - q\Big) \prod_{n=1}^{N} d^3p_n / \left((2\pi)^3 2E_n\right) , \tag{2.6}$$

where the lepton tensors $L^{\mu\nu}_r$ are defined in Appendix A, the hadron tensors $H^{\mu\nu}_r$ in Apendix B and L·H stands for $L^{\mu\nu}H_{\mu\nu}$. The coefficients $g^f_{r'r}$ depend only on s and on the coupling constants entering (2.4). They contain all the information on γ-Z-interference and on the Z^0-boson itself and are given explicitly by

$$g^f_{11} = Q_e^2 Q_f^2 + 2Q_e Q_f v v_f \,\mathrm{Re}\,\chi_Z + (v^2+a^2)(v_f^2+a_f^2)\,|\chi_Z|^2 ,$$

$$g^f_{12} = Q_e^2 Q_f^2 + 2Q_e Q_f v v_f \,\mathrm{Re}\,\chi_Z + (v^2+a^2)(v_f^2-a_f^2)\,|\chi_Z|^2 ,$$

$$g^f_{13} = 2Q_e Q_f v a_f \,\mathrm{Im}\,\chi_Z ,$$

$$g^f_{14} = -\left[2Q_e Q_f v a_f \,\mathrm{Re}\,\chi_Z + (v^2+a^2)\, 2v_f a_f\, |\chi_Z|^2\right] ;$$

$$g^f_{21} = Q_e^2 Q_f^2 + 2Q_e Q_f v v_f \,\mathrm{Re}\,\chi_Z + (v^2-a^2)(v_f^2+a_f^2)\,|\chi_Z|^2 ,$$

$$g^f_{22} = Q_e^2 Q_f^2 + 2Q_e Q_f v v_f \,\mathrm{Re}\,\chi_Z + (v^2-a^2)(v_f^2-a_f^2)\,|\chi_Z|^2 ,$$

$$g^f_{23} = g^f_{13} ,$$

$$g^f_{24} = -\left[2Q_e Q_f v a_f \,\mathrm{Re}\,\chi_Z + (v^2-a^2)\, 2v_f a_f\, |\chi_Z|^2\right] ;$$

$$g^f_{31} = 2Q_e Q_f a v_f \,\mathrm{Im}\,\chi_Z ,$$

$$g^f_{32} = g^f_{31} ,$$

$$g^f_{33} = -2Q_e Q_f a a_f \,\mathrm{Re}\,\chi_Z ,$$

$$g^f_{34} = -2Q_e Q_f a a_f \,\mathrm{Im}\,\chi_Z ;$$

$$g^f_{41} = -\left[2Q_e Q_f a v_f \,\mathrm{Re}\,\chi_Z + 2va(v_f^2+a_f^2)\,|\chi_Z|^2\right] ,$$

$$g^f_{42} = -\left[2Q_e Q_f a v_f \,\mathrm{Re}\,\chi_Z + 2va(v_f^2-a_f^2)\,|\chi_Z|^2\right] ,$$

$$g^f_{43} = g^f_{34}$$

$$g^f_{44} = 2Q_e Q_f a a_f \,\mathrm{Re}\,\chi_Z + 4va\, v_f a_f\, |\chi_Z|^2 . \tag{2.7}$$

We note the symmetry relations (with $v = v_e$, $a = a_e$)

$$g^f_{r'r} = g^f_{rr'}(e \leftrightarrow f) \tag{2.8}$$

and observe that g^f_{11} is nothing else than the ratio $R_f = \sigma(e^-e^+ \to \gamma, Z \to f\bar{f})/\sigma(e^-e^+ \to \gamma \to \mu^-\mu^+)$ of the total cross sections for the indicated binary reactions [7]. It is then sensible to introduce the normalized parameters

$$A^f_{r'r}(s) = g^f_{r'r}(s) / g^f_{11}(s) , \tag{2.9}$$

most of which are related to angular asymmetries (contained in $L_{r'} \cdot H^f_r$)and can be determined thereof.

In the 1γ-exchange approximation all coefficients $g^f_{r'r}$ vanish except $g^f_{11} = g^f_{12} = g^f_{21} = g^f_{22} = Q^2_f$, so that

$$\sum_{r',r=1}^{4} g^f_{r'r}(s)\, L_{r'} \cdot H^f_r \xrightarrow[1\gamma]{} Q^2_f\, L_{jj} \cdot H^f_{JJ} , \tag{2.10}$$

in agreement with our previous result [10]. Using (2.10) in the opposite direction, we have a nice substitution rule for going from $\sigma(1\gamma)$ to $\sigma(1\gamma, 1Z^0)$.

In order to exhibit the various angular distributions contained in (2.6) we find it convenient to shift all angular dependences into the explicitly known lepton tensors. The hadron tensors then become independent of the overall orientation in space of a given final state configuration. We introduce in the center of mass system of the colliding beams ($\vec{q} = \vec{p}_- + \vec{p}_+ = 0$) two reference frames Ox'y'z' and Oxyz rigidly fixed to the initial and final state, respectively, the common origin O being the interaction point. We call, in analogy to classical mechanics, Ox'y'z' the space-fixed frame and Oxyz the body-fixed one. Oxyz is obtained from Ox'y'z' by a rotation $R(\varphi,\theta,\chi)$ through Euler angles φ, θ and χ (Fig.2) For definiteness we choose Oz' pointing into the direction of the electron-beam and Ox' into that of the Lorentz force. To fix the frame Oxyz any two noncolinear final state momenta can be chosen.

Consider now the quantities $L \cdot H = L^{\mu\nu} H_{\mu\nu}$ appearing in (2.6). Since we neglect the electron mass, all lepton tensors $L^{\mu\nu}$ have $L^{oo} = L^{on} = L^{mo} = 0$ for $m,n = 1,2,3$. Then $L^{\mu\nu} H_{\mu\nu}$ reduces to $L^{mn} H_{mn}$ and this rotationally invariant quantity can be evaluated either in Ox'y'z', or in Oxyz. In the first case the lepton tensors are very simple, see (A.6), but the hadron tensors depend explicitly on φ,θ,χ. In the second case the dependence on φ,θ,χ comes in through the lepton tensors, see (A.8), whereas the hadron tensors depend only on internal variables, like energies and relative angles. In this case we can use the results of Appendix A to write (see (A.11))

$$\begin{aligned}
\tfrac{3}{4} L_1 \cdot H^f_r &= (1-h^-h^+)\,\hat{\sigma}^f_{Ar} + (h^- - h^+)\,\hat{\sigma}^f_{Dr} , \\
\tfrac{3}{4} L_2 \cdot H^f_r &= X(\varphi)\,\hat{\sigma}^f_{Br} + Y(\varphi)\,\hat{\sigma}^f_{Cr} , \\
\tfrac{3}{4} L_3 \cdot H^f_r &= X(\varphi)\,\hat{\sigma}^f_{Cr} - Y(\varphi)\,\hat{\sigma}^f_{Br} , \\
\tfrac{3}{4} L_4 \cdot H^f_r &= (1-h^-h^+)\,\hat{\sigma}^f_{Dr} + (h^- - h^+)\,\hat{\sigma}^f_{Ar} , \qquad r = 1,2,3,4,
\end{aligned} \tag{2.11}$$

where $h^\pm$ is the longitudinal $e^\pm$-beam polarization (A.5), $X(\varphi)$ and $Y(\varphi)$ are related by (A.12) or (A.13) to the transverse beam polarization, and

$$\hat{\sigma}^f_{Kr} = \sum_{\alpha=1}^{9} d_{K\alpha}(\theta,\chi)\,\hat{\sigma}_\alpha(H^f_r) , \qquad K = A,B,C,D. \tag{2.12}$$

This is a matrix notation of (A.10) with $\alpha = 1,2,3$ for U,L,T and with $d_{K\alpha}(\theta,\chi)$ the angular coefficients appearing there. The quantities $\hat{\sigma}_\alpha(H^f_r)$ are defined in (B.3) in terms of the components $(H^f_r)_{mn}$ refering to the body-fixed frame Oxyz and thus not containing any dependence on φ,θ and χ.

Regarding the phase-space factor in (2.6) we express it in terms of the total four-momentum q^μ, the Euler angles φ, θ and χ, and a set of 3N-7 "internal" variables $\{x\} = \{x_1, x_2, \dots, x_{3N-7}\}$ like energies and/or relative angles $\hat{p}_k \cdot \hat{p}_\ell = \cos\theta_{k\ell}$. For this change of variables we write

$$\delta_4\Big(\sum_{n=1}^{N} p_n - q\Big)\,(2\pi)^7\,\frac{2}{s}\prod_{n=1}^{N}\frac{d^3p_n}{(2\pi)^3\,2E_n}$$

$$\longrightarrow J\,d\varphi\,d\cos\theta\,d\chi\,d\{x\}\ , \qquad (2.13)$$

where J is the corresponding Jacobian which does not depend on φ, θ and χ, but may depend on q^2 and $\{x\}$.

Using now (2.11) and (2.13) in (2.6) and introducing the notations

$$\sigma^f_{\alpha r} = \frac{d^{3N-7}\sigma^f_{\alpha r}}{d\{x\}} = J\,\hat{\sigma}_\alpha\,(H^f_r)\ , \qquad \alpha = 1,2,\dots,9\ , \qquad (2.14)$$

$$\sigma^f_{Kr} = \sum_{\alpha=1}^{9} d_{K\alpha}(\theta,\chi)\,\sigma^f_{\alpha r}\ , \qquad K = A,B,C,D, \qquad (2.15)$$

for r = 1,2,3 and 4, the differential cross section for the process depicted in Fig. 1 can be written in the following form

$$\frac{(2\pi)^2}{\sigma_{pt}}\,\frac{d^{3N-4}\sigma^f}{d\varphi\,d\cos\theta\,d\chi\,d\{x\}} = (1-h^-h^+)\,\tau^f + X(\varphi)\,T^f_{11} + Y(\varphi)\,T^f_{12} + (h^- - h^+)\,T^f_3\ , \qquad (2.16)$$

where $\sigma_{pt} = 4\pi\alpha^2/3s$ is the point-like cross section for $e^-e^+ \to \gamma \to \mu^-\mu^+$ and the quantities

$$\tau^f = \sum_{r=1}^{4}\big(g^f_{1r}\,\sigma^f_{Ar} + g^f_{4r}\,\sigma^f_{Dr}\big)\ ,$$

$$T^f_{11} = \sum_{r=1}^{4}\big(g^f_{2r}\,\sigma^f_{Br} + g^f_{3r}\,\sigma^f_{Cr}\big)\ ,$$

$$T^f_{12} = \sum_{r=1}^{4}\big(g^f_{2r}\,\sigma^f_{Cr} - g^f_{3r}\,\sigma^f_{Br}\big)\ ,$$

$$T^f_3 = \sum_{r=1}^{4}\big(g^f_{1r}\,\sigma^f_{Dr} + g^f_{4r}\,\sigma^f_{Ar}\big) \qquad (2.17)$$

are related, respectively, to the cross section for unpolarized beams, for transversely ($X(\varphi)$, $Y(\varphi)$) and longitudinally ($h^\pm$) polarized beams. The coefficients $g^f_{r'r}$ are given by (2.7). Using (2.9) and noting that $\sigma_{pt}\,g^f_{11} = \sigma_{f\bar f}$ is just the total cross section for the binary reaction $e^-e^+ \to \gamma, Z \to f\bar f$, we get the cross section (2.16) normalized to $\sigma_{f\bar f}$ (instead to σ_{pt}) by simply replacing $g^f_{r'r} \to A^f_{r'r}$ in (2.17).

The cross section (2.16) has a rather "factorized" structure: i) the angular dependences which merely reflect the spin-one nature of the virtual γ and Z^0 are contained in $X(\varphi)$, $Y(\varphi)$ and $d_{K\alpha}(\theta,\chi)$, ii) the polarization of the beams in $X(\varphi = 0)$, $Y(\varphi = 0)$ and $h^\pm$, iii) the couplings of the Z^0 in $g^f_{r'r}(s)$ and iv) the properties of the final state (e.g. QCD effects in case $f\bar f$ is a quark-antiquark pair) in $\sigma^f_{\alpha r}$. This has the big advantage that for different final states one must not go through the whole "zedology" each time. Only the cross sections $\sigma^f_{\alpha r}$ (2.14) have to be computed from the Jacobian (2.13) and, according to (B.3), from the hadron tensors $(H^f_r)_{mn}$ evaluated in the body-fixed frame Oxyz (no φ,θ,χ-dependence!). In section 4 we shall consider the final state $q\bar q g$ as an example.

It is sometimes useful to have the cross section (2.16) written in the form

$$\frac{(2\pi)^2}{\sigma_{pt}}\,\frac{d^{3N-4}\sigma^f}{d\varphi\,d\cos\theta\,d\chi\,d\{x\}} = \sum_{r=1}^{4}\Big\{G^f_{Ar}\,\sigma^f_{Ar}$$

$$+\big(G^f_{Br}\,\sigma^f_{Br} + G^f_{Cr}\,\sigma^f_{Cr}\big)\cos 2\varphi + \big(G^f_{Cr}\,\sigma^f_{Br} - G^f_{Br}\,\sigma^f_{Cr}\big)\sin 2\varphi + G^f_{Dr}\,\sigma^f_{Dr}\Big\}, \qquad (2.18)$$

where the G^f_{Kr}'s are defined by

$$G^f_{Ar} = (1-h^-h^+)\,g^f_{1r} + (h^- - h^+)\,g^f_{4r}\ ,$$

$$G^f_{Br} = \big(\xi^-_{x'}\xi^+_{x'} - \xi^-_{y'}\xi^+_{y'}\big)\,g^f_{2r} - \big(\xi^-_{x'}\xi^+_{y'} + \xi^-_{y'}\xi^+_{x'}\big)\,g^f_{3r}\ ,$$

$$G^f_{Cr} = \big(\xi^-_{x'}\xi^+_{x'} - \xi^-_{y'}\xi^+_{y'}\big)\,g^f_{3r} + \big(\xi^-_{x'}\xi^+_{y'} + \xi^-_{y'}\xi^+_{x'}\big)\,g^f_{2r}\ ,$$

$$G^f_{Dr} = (1-h^-h^+)\,g^f_{4r} + (h^- - h^+)\,g^f_{1r}\ . \qquad (2.19)$$

Some of these coefficients allready appear in the angular distribution of the binary reaction $e^-e^+ \to \gamma, Z \to f\bar{f}$, namely G_{A1}, G_{B1}, G_{C1} and G_{D4} (denoted, respectively, by G_1, G_3, G_4 and G_5 in [7]). In (2.18) the θ,χ-dependence is still hidden in σ^f_{Kr}. Using (2.15) and defining the quantities $S^f_{K\alpha}$ by

$$S^f_{K\alpha} = \sum_{r=1}^{4} G^f_{Kr}\, \sigma^f_{\alpha r} \tag{2.20}$$

(K = A, B, C, D; α = 1, 2, ..., 9), the cross section (2.18) can be written as

$$\frac{(2\pi)^2}{\sigma_{pt}} \frac{d^{3N-4}\sigma^f}{d\varphi\, d\cos\theta\, d\chi\, d\{x\}} = \sum_{\alpha=1}^{6} \Big\{ d_{A\alpha}(\theta,\chi)\, S^f_{A\alpha} + \left[\cos 2\varphi\, d_{B\alpha}(\theta,\chi) - \sin 2\varphi\, d_{C\alpha}(\theta,\chi)\right] S^f_{B\alpha} + \left[\sin 2\varphi\, d_{B\alpha}(\theta,\chi) + \cos 2\varphi\, d_{C\alpha}(\theta,\chi)\right] S^f_{C\alpha} \Big\} + \sum_{\alpha=7}^{9} d_{D\alpha}(\theta,\chi)\, S^f_{D\alpha} \,, \tag{2.21}$$

(compare (2.12) and (A.10) for the definition of $d_{K\alpha}$). This expression exhibits the whole angular dependence, since the "cross sections" $S^f_{K\alpha}$ do not depend on φ,θ,χ. They depend only on the beam polarization and properties of the Z^o (through G^f_{Kr}) and on the dynamics of the final state (through $\sigma^f_{\alpha r}$).

The angular distribution of the body-fixed $\hat{z}$-axis is just the θ,φ-distribution given by

$$\frac{(2\pi)}{\sigma_{pt}} \frac{d^{3N-5}\sigma^f}{d\varphi\, d\cos\theta\, d\{x\}} = \frac{3}{8}\left(S^f_{AU} + 2S^f_{AL}\right)\Big\{ 1 + \alpha^f_A \cos^2\theta + \alpha^f_B \sin^2\theta \cos 2\varphi + \alpha^f_C \sin^2\theta \sin 2\varphi + 2\epsilon^f_7 \cos\theta \Big\}, \tag{2.22}$$

where we have defined

$$\alpha^f_K = \left(S^f_{KU} - 2S^f_{KL}\right)/\left(S^f_{AU} + 2S^f_{AL}\right), \qquad K = A, B, C\,,$$

$$\epsilon^f_7 = S^f_{D7}/\left(S^f_{AU} + 2S^f_{AL}\right). \tag{2.23}$$

Here $\alpha^f_K(\epsilon^f_7)$ receive contribution from the real (imaginary) part of the hadron tensors only. Furthermore α^f_A, $\epsilon^f_7(\alpha^f_B, \alpha^f_C)$ depend only on the longitudinal (transverse) beam polarization. The last term in (2.22) gives rise to a forward-backward asymmetry of the $\hat{z}$-axis

$$A^f_{FB} = \frac{3}{2}\langle\cos\theta\rangle^f = \frac{3}{4}\frac{S^f_{D7}}{S_{AU} + S_{AL}} \,, \tag{2.24}$$

where the denominator is just the angle-integrated cross section

$$\frac{1}{\sigma_{pt}} \frac{d^{3N-7}\sigma^f}{d\{x\}} = S^f_{AU} + S^f_{AL} = J \sum_{r=1}^{4} G^f_{Ar}\left(\sum_{m=1}^{3} H^{mm}_r\right) \tag{2.25}$$

(J from (2.13)), given by G^f_{Ar} and the rotationally invariant traces of the hadron tensors (B.2).

Another interesting angular distribution is the θ,χ-distribution resulting from (2.21)

$$\frac{(2\pi)}{\sigma_{pt}} \frac{d^{3N-5}\sigma^f}{d\cos\theta\, d\chi\, d\{x\}} = \frac{3}{8}\left(S^f_{AU} + 2S^f_{AL}\right)\Big\{ 1 + \alpha^f_A \cos^2\theta + \alpha^f_3 \sin^2\theta \cos 2\chi + \alpha^f_4 \sin^2\theta \sin 2\chi + \alpha^f_5 \sin 2\theta \sin\chi + \alpha^f_6 \sin 2\theta \cos\chi + 2\epsilon^f_7 \cos\theta + \epsilon^f_8 \sin\theta \cos\chi + \epsilon^f_9 \sin\theta \sin\chi \Big\}. \tag{2.26}$$

Here we have defined in addition to (2.23) the χ-related asymmetry parameters

$$\alpha_\alpha^f = \delta_\alpha S_{A\alpha}^f / (S_{AU} + 2S_{AL}) , \qquad \alpha = 3,4,5,6,$$
$$\epsilon_\alpha^f = \delta_\alpha S_{D\alpha}^f / (S_{AU} + 2S_{AL}) , \qquad \alpha = 8,9, \tag{2.27}$$

with δ_α = 2, -2, $2\sqrt{2}$, $-2\sqrt{2}$, $-4\sqrt{2}$, $4\sqrt{2}$ for α = 3,4,5,6,8 and 9 respectively. Here $\alpha_\alpha^f(\epsilon_\alpha^f)$ get contributions from the real (imaginary) part of the hadron tensors only and may depend on longitudinal beam polarization.

Besides the angular asymmetries (2.23) and (2.27) there is the polarization asymmetry

$$\mathcal{P}^f = \frac{d\sigma^f(h) - d\sigma^f(-h)}{d\sigma^f(h) + d\sigma^f(-h)} = h\,\frac{T_3^f}{\tau^f} , \qquad h = \frac{h^- - h^+}{1 - h^- h^+} \tag{2.28}$$

related to longitudinal beam polarization and picking up parity-odd contributions to the cross section.

The angular distributions considered so far simplify very much in the 1γ-exchange approximation (no Z^0). Remembering (2.10) we may do either the substitutions

$$\tau^f \rightarrow Q_f^2\,\sigma_A(H_{JJ}^f) , \qquad T_3^f \rightarrow Q_f^2\,\sigma_D(H_{JJ}^f),$$
$$T_{11}^f \rightarrow Q_f^2\,\sigma_B(H_{JJ}^f) , \qquad T_{12}^f \rightarrow Q_f^2\,\sigma_C(H_{JJ}^f) \tag{2.29}$$

in (2.16), or the substitutions

$$\left.\begin{array}{l} S_{A\alpha}^f \longrightarrow (1 - h^- h^+) \\ S_{B\alpha}^f \longrightarrow (\xi_{x'}^- \xi_{x'}^+ - \xi_{y'}^- \xi_{y'}^+) \\ S_{C\alpha}^f \longrightarrow (\xi_{x'}^- \xi_{y'}^+ + \xi_{y'}^- \xi_{x'}^+) \\ S_{D\alpha}^f \longrightarrow (h^- - h^+) \end{array}\right\} \times Q_f^2\,\sigma_\alpha(H_{JJ}^f) \quad \begin{array}{l} \left.\right\}\ \alpha = 1,2,\dots,6 \\ \\ \alpha = 7,8,9 \end{array} \tag{2.30}$$

in (2.21) - (2.28). Here $\sigma_\alpha(H_{JJ}^f) = J\partial_\alpha(H_{JJ}^f)$ with $\partial_\alpha(H_{JJ}^f)$ given by (B.3) for $H = H_{JJ}^f$. Now the angular asymmetries related to $S_{D\alpha}^f$ show up only for longitudinally polarized beams. Moreover, since $S_{D\alpha}^f$ receive contribution from the imaginary part of the electromagnetic hadron tensor only, they usually vanish unless final state interactions and/or spin effects are taken into account.

For the θ,φ-related asymmetry parameters (2.23) we get from (2.30) in the 1γ-exchange approximation ($\sigma_\alpha^f = \sigma_\alpha(H_{JJ}^f)$)

$$\alpha_A^f \longrightarrow \alpha_f = (\sigma_U^f - 2\sigma_L^f)/(\sigma_U^f + 2\sigma_L^f) ,$$
$$\alpha_B \longrightarrow \alpha_f\,(\xi_{x'}^- \xi_{x'}^+ - \xi_{y'}^- \xi_{y'}^+)/(1 - h^- h^+) ,$$
$$\alpha_C \longrightarrow \alpha_f\,(\xi_{x'}^- \xi_{y'}^+ + \xi_{y'}^- \xi_{x'}^+)/(1 - h^- h^+) ,$$
$$\epsilon_7^f \longrightarrow \epsilon_f\,(h^- - h^+)/(1 - h^- h^+) , \qquad \epsilon_f = \sigma_7^f/(\sigma_U^f + 2\sigma_L^f) , \tag{2.31}$$

where α_f and ϵ_f are the parameters already used in 1γ-physics. For naturally polarized beams ($\xi_{x'}^\pm = 0$, $\xi_{y'}^\pm = \pm P$, $h^\pm = 0$) we obtain

$$\alpha_A^f \rightarrow \alpha_f , \quad \alpha_B^f \rightarrow P^2 \alpha_f , \quad \alpha_C^f \rightarrow 0 , \quad \epsilon_7^f \rightarrow 0 \tag{2.32}$$

and (2.22) reduces to the well-known expression used, e.g. for the angular distribution of the jet axis. The Z^0-boson would modify the result (2.32) according to

$$\alpha_A^f = [\Sigma g_{1r}^f (\sigma_{Ur}^f - 2\sigma_{Lr}^f)]\,[\Sigma g_{1r}^f (\sigma_{Ur}^f + 2\sigma_{Lr}^f)]^{-1}$$
$$\alpha_B^f = P^2 [\,\Sigma g_{2r}^f (\sigma_{Ur}^f - 2\sigma_{Lr}^f)][\,\Sigma g_{1r}^f (\sigma_{Ur}^f + 2\sigma_{Lr}^f)]^{-1} ,$$
$$\alpha_C^f = P^2 [\,\Sigma g_{3r} (\sigma_{Ur}^f - 2\sigma_{Lr}^f)][\,\Sigma g_{1r}^f (\sigma_{Ur}^f + 2\sigma_{Lr}^f)]^{-1} ,$$
$$\epsilon_7^f = [\,\Sigma g_{4r}^f\,\sigma_{7r}^f\,][\,\Sigma g_{1r}^f (\sigma_{Ur}^f + 2\sigma_{Lr}^f)\,]^{-1} \tag{2.33}$$

(all sums over r = 1, 2, 3, 4). These relations show that in the case of naturally polarized beams the coefficients $g^f_{r'r}$ (2.7) are simply related to the parameters α^f_K and ϵ^f_7 entering the angular distribution (2.22) of the body-fixed $\hat{z}$-axis. The χ-related asymmetry parameters (2.27) become in the 1γ-exchange approximation

$$\begin{aligned} \alpha^f_\alpha &\rightarrow \delta_\alpha \sigma_\alpha^f/(\sigma_U^f + 2\sigma_L^f)\,, \qquad \alpha = 3,4,5,6 \\ \epsilon^f_\alpha &\rightarrow h\,\delta_\alpha \sigma_\alpha^f/(\sigma_U^f + 2\sigma_L^f)\,, \qquad \alpha = 8,9\,, \end{aligned} \tag{2.34}$$

whereas the polarization asymmetry (2.28) is now given by

$$\mathcal{P}^f \rightarrow h\,\sigma_D(H^f_{JJ})/\sigma_A(H^f_{JJ}). \tag{2.35}$$

The angular asymmetries related with ϵ^f_α (α = 7, 8, 9) and thus with the imaginary part of the hadron tensors are present, in the 1γ-exchange approximation, only for longitudinally polarized beams. If Z^0-exchange is included, these asymmetries survive even for unpolarized beams due to the axial couplings of the Z^0. But londigutinal beam polarization may still be very helpful as it introduces, according to (2.18) and (2.19), the usually "small" σ^f_{Dr} along with the "large" g^f_{1r}, and the "small" g^f_{4r} along with the "large" σ^f_{Ar}. Compared with the unpolarized case, when only the combination $g^f_{4r}\,\sigma^f_{Dr}$ appears, this may give us a better chance to learn something about the small, but interesting quantities g^f_{4r} and σ^f_{Dr}.

3. Planar events

In this section we discuss the angular distributions of planar events for which the final state is symmetric with respect to a plane called event plane. For a three-particle final state (or 3-jet event) this is always the case, but it may happen also for multi-particle final states (or multi-jet events with vanishing aplanarity). In the case of planar events the angular distributions considered in the last section considerably simplify due to the additional mirror symmetry with respect to the event plane. Depending on the way we relate our body-fixed frame Oxyz of Fig. 2 to the event plane we get different distributions which fall into two classes:

a) Helicity-frame distributions, for which the event plane is chosen as the Oxz-plane with Oz pointing along some momentum or other direction (e.g. jet-axis) in this plane (convention C-II in [10]);

b) Transversity-frame distributions, for which the event plane is chosen as the Oxy-plane with Oz along the normal to the event plane (convention C-I in [10]).

In Fig. 3 we show possible choices of an helicity- and transversity-frame. The advantage of our method presented in section 2 becomes now evident. Since, by definition, the Euler angles φ and θ always determine the direction of Oz in the frame Ox'y'z' (Fig.2), we automatically get the angular distribution of some particle or of the jet-axis in case a), and of the normal to the event plane in case b). The physical meaning of the Euler angles is however different in the two cases (see below).

3a) Helicity-frame distributions.

In this case the event plane is chosen as the Oxz-plane of our body-fixed frame Oxyz so that reflection in this plane means $\hat{y} \rightarrow -\hat{y}$. Under this reflection a vector $\vec{J}$ and an axial-vector $\vec{A}$ transform according to

$$\begin{aligned} (J_x, J_y, J_z) &\longrightarrow (J_x, -J_y, J_z)\,, \\ (A_x, A_y, A_z) &\longrightarrow (-A_x, A_y, -A_z). \end{aligned} \tag{3.1}$$

Invariance under this symmetry operation then implies for the hadron tensors H_r^{mn} in (B.1) - (B.2):

$$r = 1,2 \;:\quad H_r^{12} = H_r^{21} = H_r^{23} = H_r^{32} = 0 ,$$

$$r = 3,4 \;:\quad H_r^{11} = H_r^{22} = H_r^{33} = H_r^{13} = H_r^{31} = 0. \tag{3.2}$$

According to (B.3) and (2.14) this means

$$r = 1,2 :\quad \sigma_{4r} = \sigma_{5r} = \sigma_{7r} = \sigma_{8r} = 0 ,$$

$$r = 3,4 :\quad \sigma_{Ur} = \sigma_{Lr} = \sigma_{Tr} = \sigma_{6r} = \sigma_{9r} = 0 , \tag{3.3}$$

i.e. H_1, H_2 and H_3, H_4 contribute (complementarily) to different cross sections. For σ^f_{Kr} in(2.15) we then obtain (with the usual notation $\sigma_I = \sigma_6$):

$$\begin{aligned}
\sigma^f_{Ar} &= \tfrac{3}{8}(1+\cos^2\theta)\,\sigma^f_{Ur} + \tfrac{3}{4}\sin^2\theta\,\sigma^f_{Lr} + \tfrac{3}{4}\sin^2\theta\cos 2\chi\,\sigma^f_{Tr} - \tfrac{3}{2\sqrt{2}}\sin 2\theta\cos\chi\,\sigma^f_{Ir} ,\\
\sigma^f_{Br} &= \tfrac{3}{8}\sin^2\theta\,\sigma^f_{Ur} - \tfrac{3}{4}\sin^2\theta\,\sigma^f_{Lr} + \tfrac{3}{4}(1+\cos^2\theta)\cos 2\chi\,\sigma^f_{Tr} + \tfrac{3}{2\sqrt{2}}\sin 2\theta\cos\chi\,\sigma^f_{Ir} ,\\
\sigma^f_{Cr} &= \tfrac{3}{2}\cos\theta\sin 2\chi\,\sigma^f_{Tr} + \tfrac{3}{\sqrt{2}}\sin\theta\sin\chi\,\sigma^f_{Ir} ,\\
\sigma^f_{Dr} &= \tfrac{3}{\sqrt{2}}\sin\theta\sin\chi\,\sigma^f_{9r}
\end{aligned} \tag{3.4}$$

for $r = 1,2$, and

$$\begin{aligned}
\sigma^f_{Ar} &= -\tfrac{3}{4}\sin^2\theta\sin 2\chi\,\sigma^f_{4r} + \tfrac{3}{2\sqrt{2}}\sin 2\theta\sin\chi\,\sigma^f_{5r} ,\\
\sigma^f_{Br} &= -\tfrac{3}{4}(1+\cos^2\theta)\sin 2\chi\,\sigma^f_{4r} - \tfrac{3}{2\sqrt{2}}\sin 2\theta\sin\chi\,\sigma^f_{5r} ,\\
\sigma^f_{Cr} &= \tfrac{3}{2}\cos\theta\cos 2\chi\,\sigma^f_{4r} + \tfrac{3}{\sqrt{2}}\sin\theta\cos\chi\,\sigma^f_{5r} ,\\
\sigma^f_{Dr} &= \tfrac{3}{4}\cos\theta\,\sigma^f_{7r} - \tfrac{3}{\sqrt{2}}\sin\theta\cos\chi\,\sigma^f_{8r}
\end{aligned} \tag{3.5}$$

for r = 3, 4. The general cross section is given then by using (3.4) - (3.5) in (2.16) - (2.17) or in (2.18) - (2.19). For the cross sections $S^f_{K\alpha}$ from (2.20) the conditions (3.3) imply

$$S^f_{K\alpha} = \begin{cases} \sum\limits_{r=1,2} G^f_{Kr}\,\sigma^f_{\alpha r} & \text{for } K = A,B,C \text{ and } \alpha = 1,2,3,6 ,\\ & \phantom{\text{for }} K = D \phantom{\text{ and }} \alpha = 9 ;\\ \sum\limits_{r=3,4} G^f_{Kr}\,\sigma^f_{\alpha r} & \text{for } K = A,B,C \text{ and } \alpha = 4,5 ,\\ & \phantom{\text{for }} K = D \phantom{\text{ and }} \alpha = 7,8 ;\\ 0 & \text{for all others .} \end{cases} \tag{3.6}$$

The various angular distributions are then explicitly given by (2.21) - (2.27). Note in particular that now the sums over r in (2.33) go only over r = 1, 2 for σ^f_{Ur} and σ^f_{Lr}, and over r = 3, 4 for σ^f_{7r}.

In the 1γ-exchange approximation the cross section for planar events is given, in a helicity-frame, by

$$\frac{(2\pi)^2}{\sigma_{pt}}\,\frac{d^{3N-4}\sigma^f}{d\varphi\, d\cos\theta\, d\chi\, d\{x\}} \xrightarrow[1\gamma]{} Q_f^2\Big\{(h^- - h^+)\tfrac{3}{\sqrt{2}}\sin\theta\sin\chi\;\sigma_9(H^f_{JJ})$$

$$+\sum_{\alpha=U,L,T,I}\big[(1-h^-h^+)\,d_{A\alpha}(\theta,\chi) + X(\varphi)\,d_{B\alpha}(\theta,\chi) + Y(\varphi)\,d_{C\alpha}(\theta,\chi)\big]\,\sigma_\alpha(H^f_{JJ})\Big\} , \tag{3.7}$$

with $d_{K\alpha}(\theta,\chi)$ the angular coefficients appearing in (3.4).

We finally note that the mathematical definition of the Euler angles φ, θ and χ is always according to Fig.2, but their physical meaning depends on the particular choice of the helicity-frame. Thus for the typical 3-jet event shown in Fig.3a and the choice of the helicity-frame in Fig.3b (Oz along the jet axis and Ox pointing into the half-plane of the second most energetic jet), the meaning of these angles is as follows: φ is the (azimuthal) angle (around the beam axis) between the plane of the storage ring and the "scattering plane" Oz'z determined by the beam and jet axes; θ is the (polar) angle between the beam and jet axis; χ is the (azimuthal) angle (around the jet axis) between the "scattering plane" Oz'z and the event plane Ozx. Identifying the jet axis with the thrust, sphericity or spheriocity axis we obtain in fact different helicity-frames and the angular distributions change accordingly as the hadron tensors are evaluated in different body-fixed frames [11].

3b) Transversity-frame distributions

Now the event plane is chosen as the Oxy-plane and reflection in it means $\hat{z} \to -\hat{z}$. Instead of (3.1) we now have (putting a bar on quantities refering to the transversity frame)

$$(\bar{J}_x, \bar{J}_y, \bar{J}_z) \longrightarrow (\bar{J}_x, \bar{J}_y, -\bar{J}_z),$$
$$(\bar{A}_x, \bar{A}_y, \bar{A}_z) \longrightarrow (-\bar{A}_x, -\bar{A}_y, \bar{A}_z), \tag{3.8}$$

so that invariance under (3.8) implies

$$r = 1,2 : \quad \bar{H}^{13}_r = \bar{H}^{31}_r = \bar{H}^{23}_r = \bar{H}^{32}_r = 0,$$
$$r = 3,4 : \quad \bar{H}^{11}_r = \bar{H}^{22}_r = \bar{H}^{33}_r = \bar{H}^{12}_r = \bar{H}^{21}_r = 0. \tag{3.9}$$

From (B.3)and (2.14) we then get

$$r = 1,2 : \quad \bar{\sigma}_{5r} = \bar{\sigma}_{6r} = \bar{\sigma}_{8r} = \bar{\sigma}_{9r} = 0,$$
$$r = 3,4 : \quad \bar{\sigma}_{Ur} = \bar{\sigma}_{Lr} = \bar{\sigma}_{Tr} = \bar{\sigma}_{4r} = \bar{\sigma}_{7r} = 0, \tag{3.10}$$

and from (2.15) and (A.10) (with $\bar{\sigma}_I = \bar{\sigma}_4$):

$$\bar{\sigma}^f_{Ar} = \frac{3}{8}(1+\cos^2\bar{\theta})\bar{\sigma}^f_{Ur} + \frac{3}{4}\sin^2\bar{\theta}\,\bar{\sigma}^f_{Lr} + \frac{3}{4}\sin^2\bar{\theta}\cos 2\bar{\chi}\,\bar{\sigma}^f_{Tr} - \frac{3}{4}\sin^2\bar{\theta}\sin 2\bar{\chi}\,\bar{\sigma}^f_{Ir},$$
$$\bar{\sigma}^f_{Br} = \frac{3}{8}\sin^2\bar{\theta}\,\bar{\sigma}^f_{Ur} - \frac{3}{4}\sin^2\bar{\theta}\,\bar{\sigma}^f_{Lr} + \frac{3}{4}(1+\cos^2\bar{\theta})\cos 2\bar{\chi}\,\bar{\sigma}^f_{Tr} - \frac{3}{4}(1+\cos^2\bar{\theta})\sin 2\bar{\chi}\,\bar{\sigma}^f_{Ir},$$
$$\bar{\sigma}^f_{Cr} = \frac{3}{2}\cos\bar{\theta}\sin 2\bar{\chi}\,\bar{\sigma}^f_{Tr} + \frac{3}{2}\cos\bar{\theta}\cos 2\bar{\chi}\,\bar{\sigma}^f_{Ir},$$
$$\bar{\sigma}^f_{Dr} = \frac{3}{4}\cos\bar{\theta}\,\bar{\sigma}^f_{7r} \tag{3.11}$$

for r = 1, 2, and

$$\bar{\sigma}^f_{Ar} = \frac{3}{2\sqrt{2}}\sin 2\bar{\theta}\sin\bar{\chi}\,\bar{\sigma}^f_{5r} - \frac{3}{2\sqrt{2}}\sin 2\bar{\theta}\cos\bar{\chi}\,\bar{\sigma}^f_{6r},$$
$$\bar{\sigma}^f_{Br} = -\bar{\sigma}^f_{Ar},$$
$$\bar{\sigma}^f_{Cr} = \frac{3}{\sqrt{2}}\sin\bar{\theta}\cos\bar{\chi}\,\bar{\sigma}^f_{5r} + \frac{3}{\sqrt{2}}\sin\bar{\theta}\sin\bar{\chi}\,\bar{\sigma}^f_{6r},$$
$$\bar{\sigma}^f_{Dr} = -\frac{3}{\sqrt{2}}\sin\bar{\theta}\cos\bar{\chi}\,\bar{\sigma}^f_{8r} + \frac{3}{\sqrt{2}}\sin\bar{\theta}\sin\bar{\chi}\,\bar{\sigma}^f_{9r} \tag{3.12}$$

for r = 3, 4. The general cross section for the case when the normal to the event plane is used as an analyzer then follows from (2.16) - (2.17) or (2.18) - (2.19) with σ^f_{Kr} replaced by $\bar{\sigma}^f_{Kr}$, (3,11) – (3,12). For the cross sections $\bar{S}^f_{K\alpha}$ entering the various angular distributions (2.21) - (2.27) we now obtain

$$\bar{S}^f_{K\alpha} = \begin{cases} \sum\limits_{r=1,2} G^f_{Kr}\,\bar{\sigma}^f_{\alpha r} & \text{for } K = A,B,C \text{ and } \alpha = 1,2,3,4, \\ & \phantom{\text{for }} K = D \qquad\quad\;\; \alpha = 7; \\ \sum\limits_{r=3,4} G^f_{Kr}\,\bar{\sigma}^f_{\alpha r} & \text{for } K = A,B,C \text{ and } \alpha = 5,6, \\ & \phantom{\text{for }} K = D \qquad\quad\;\; \alpha = 8,9; \\ 0 & \text{for all others.} \end{cases} \tag{3.13}$$

As a consequence all sums over r in (2.33) go only over r = 1, 2.

In the 1γ-exchange approximation the general angular distribution of the normal to the event plane is given by

$$\frac{(2\pi)^2}{\sigma_{pt}}\frac{d^{3N-4}\bar{\sigma}^f}{d\bar{\varphi}\,d\cos\bar{\theta}\,d\bar{\chi}\,d\{x\}} \xrightarrow[1\gamma]{} Q_f^2\Big\{(h^- - h^+)\frac{3}{4}\cos\bar{\theta}\,\bar{\sigma}_7(H^f_{JJ})$$
$$+ \sum_{\alpha=U,L,T,I}\Big[(1-h^-h^+)\,d_{A\alpha}(\bar{\theta},\bar{\chi}) + X(\bar{\varphi})\,d_{B\alpha}(\bar{\theta},\bar{\chi}) + Y(\bar{\varphi})\,d_{C\alpha}(\bar{\theta},\bar{\chi})\Big]\bar{\sigma}_\alpha(H^f_{JJ})\Big\} \tag{3.14}$$

where the $d_{K\alpha}(\bar\theta,\bar\chi)$'s are the angular coefficients appearing in (3.11).

The meaning of the Euler angles $\bar\varphi,\bar\theta,\bar\chi$ follows from Fig.2 and Fig. 3c. Refering again to the 3-jet event of Fig. 3a, $\bar\varphi$ is the (azimuthal) angle (around the beam axis) between the plane of the storage ring and the plane Oz'z defined by the beam axis and the normal to the event plane; $\bar\theta$ is the (polar) angle between the beam axis and the normal; $\bar\chi$ is the (azimuthal) angle (around the normal) between the plane Oz'z and the plane Ozx defined by the normal and the jet axis. By choosing Ox along some other direction in the event plane we obtain different transversity frames.

Actually there is no need to evaluate the cross sections $\bar\sigma_\alpha$ independently, once the cross sections σ_α in the helicity frame are known. As can be seen from Fig. 3b, c, the transversity frame $O\bar x\bar y\bar z$ is obtained from the helicity frame Oxyz by an Euler notation $R(-\frac{\pi}{2}, -\frac{\pi}{2}, 0)$. The components $\bar H^{mn}$ and $H^{k\ell}$ of the hadron tensor, refering to the frame $O\bar x\bar y\bar z$ and Oxyz respectively, are then related by $\bar H^{mn} = R^{km} R^{\ell n} H^{k\ell}$. Taking $R(-\frac{\pi}{2},-\frac{\pi}{2},0)$ from (A.7) and defining $\sigma_\alpha(\bar\sigma_\alpha)$ in terms of $H_{k\ell}(\bar H_{mn})$ according to (B.3), we obtain the following relations between the cross sections in the helicity and transversity frame:

$$
\begin{aligned}
\bar\sigma_U &= \tfrac{1}{2}(\sigma_U + \sigma_L - \sigma_T\;, \\
\bar\sigma_L &= \tfrac{1}{2}\sigma_U + \sigma_T\;, \\
\bar\sigma_T &= \tfrac{1}{4}\sigma_U - \tfrac{1}{2}\sigma_L - \tfrac{1}{2}\sigma_T\;, \\
\bar\sigma_4 &= \sqrt{2}\,\sigma_6\;, \\
\bar\sigma_5 &= \tfrac{1}{\sqrt{2}}\,\sigma_4\;, \\
\bar\sigma_6 &= \sigma_5\;, \\
\bar\sigma_7 &= 2\sqrt{2}\,\sigma_9\;, \\
\bar\sigma_8 &= \tfrac{1}{2\sqrt{2}}\,\sigma_7\;, \\
\bar\sigma_9 &= \sigma_8\;.
\end{aligned}
\tag{3.15}
$$

It is thus sufficient to know σ_α; in particular (3.10) simply follows from (3.3). The same relations (3.15) also hold between $\bar S^f_{K\alpha}$ (3.13) and $S^f_{K\alpha}$ (3.6) and can be used to express the angular distribution of the normal to the event plane directly in terms of the helicity cross sections $S^f_{K\alpha}$. As an example consider the distribution (2.22) integrated over $\bar\varphi$

$$
\begin{aligned}
\frac{1}{\sigma_{pt}}\frac{d^{3N-6}\,\bar\sigma^f}{d\cos\bar\theta\, d\{x\}} &= \frac{3}{8}\Big\{(\bar S^f_{AU} + 2\bar S^f_{AL}) + (\bar S^f_{AU} - 2\bar S^f_{AL})\cos^2\bar\theta + 2\bar S^f_{D7}\cos\bar\theta\Big\} \\
&= \frac{3}{8}\Big\{\left(1+\tfrac{1}{2}\sin^2\bar\theta\right)S^f_{AU} + 2\left(1-\tfrac{1}{2}\sin^2\bar\theta\right)S^f_{AL} \\
&\qquad + 2\left(-1+\tfrac{3}{2}\sin^2\bar\theta\right)S^f_{AT} + 4\sqrt{2}\cos\bar\theta\; S^f_{D9}\Big\}\;,
\end{aligned}
\tag{3.16}
$$

where $\bar\theta$ is the angle between the normal and the e^--beam. Thus the helicity cross section S^f_{D9} can be determined from the forward-backward asymmetry of the normal to the event plane. In a helicity-typ analysis the determination of S^f_{D9} would require to measure, according to (3.4), the $\sin\theta\,\sin\chi$-term in the double-differential cross section $d^2\sigma/d\cos\theta\, d\chi$. On the other hand the cross section $S^f_{D7} = 2\sqrt{2}\,\bar S^f_{D8}$, for example, can be determined either from the $\cos\theta$-term in $d\sigma/d\cos\theta$ or from the $\sin\bar\theta\cos\bar\chi$-term in $d^2\bar\sigma/d\cos\bar\theta\, d\bar\chi$, compare (3.5) and (3.12). In this case a helicity-type analysis, e.g. the $\cos\theta$-distribution of the jet-axis is preferable. It is precisely this way that helicity-type and transversity-type analyses can be combined in order to determine the cross sections $S^f_{K\alpha}$ with higher statistics.

4. Application to $e^-e^+ \to q\bar{q}g$

In the preceding sections we have worked out the general formulas for the cross section $e^-e^+ \to \gamma, Z \to F$, where F is an arbitrary final state originating in a fermion-antifermion pair $f\bar{f}$ to which the γ and Z^o directly couple (Fig.1). The results have been brought into a form which displays in a rather factorized manner the dependences on the properties and couplings of the Z^o, on beam polarization and on the dynamics of the final states. The latter is contained only in the cross sections $\sigma^f_{\alpha r}$ (2.14) which have to be calculated for each final state on the basis of the dynamics governing that state. The rest then simply follows by substituting $\sigma^f_{\alpha r}$ into the explicitly given expressions for the various angular distributions. In this section we apply our method to 3-jet events originating in a quark-antiquark pair and a gluon.

4a) The cross sections $\sigma^f_{\alpha r}$.

We now consider e^+e^- annihilation into a final state consisting of a quark-antiquark pair and a gluon

$$e^-(p_-) + e^+(p_+) \to \gamma, Z(q) \to q_{f\alpha}(p_1) + \bar{q}_{f\beta}(p_2) + g_j(p_3), \tag{4.1}$$

where f is a flavour index, α, β = 1, 2, 3 and j = 1, 2, ...,8 are SU(3)-colour indices and the momenta are indicated in parantheses. The Feynman rules for QCD lead to a matrix element of the form (2.4) with J^μ_f and A^μ_f given, in lowest order QCD, by

$$J^\mu_f = g_s\left(\frac{\lambda^j}{2}\right)_{\alpha\beta} \bar{u}_f(p_1)\, O^{\rho\mu}_f\, v_f(p_2)\, \overset{*}{\epsilon}{}^j_\rho(p_3),$$

$$A^\mu_f = g_s\left(\frac{\lambda^j}{2}\right)_{\alpha\beta} \bar{u}_f(p_1)\, O^{\rho\mu}_{5f}\, v_f(p_2)\, \overset{*}{\epsilon}{}^j_\rho(p_3), \tag{4.2}$$

where g_s is the strong coupling constant, λ^j are the Gell-Mann matrices for SU(3)-colour (there is no sum over α, β and j), $\bar{u}$, v and ϵ^j_ρ are the wave functions of q, $\bar{q}$ and g respectively, and we have defined

$$O^{\rho\mu}_f = (2p_1\cdot p_3)^{-1}\gamma^\rho(\not{p}_1+\not{p}_3+m_f)\gamma^\mu - (2p_2\cdot p_3)^{-1}\gamma^\mu(\not{p}_2+\not{p}_3-m_f)\gamma^\rho,$$

$$O^{\rho\mu}_{5f} = (2p_1\cdot p_3)^{-1}\gamma^\rho(\not{p}_1+\not{p}_3+m_f)\gamma^\mu\gamma_5 - (2p_2\cdot p_3)^{-1}\gamma^\mu\gamma_5(\not{p}_2+\not{p}_3-m_f)\gamma^\rho. \tag{4.3}$$

With J^μ_f and A^μ_f from (4.2) the hadron tensors in (B.1) can be written down easily. The bar indicated in (B.1) means in our case: summation over the spin orientations of q, $\bar{q}$ and g, and over the colour indices α, β, j ($\to$colour factor = 4). We then get

$$H^{\mu\nu}_{JJ} = -16\pi\alpha_s g_{\rho\sigma} \mathrm{Tr}\left[O^{\rho\mu}_f(\not{p}_2-m_f)\overline{O^{\sigma\nu}_f}(\not{p}_1+m_f)\right],$$

$$H^{\mu\nu}_{AA} = -16\pi\alpha_s g_{\rho\sigma} \mathrm{Tr}\left[O^{\rho\mu}_{5f}(\not{p}_2-m_f)\overline{O^{\sigma\nu}_{5f}}(\not{p}_1+m_f)\right],$$

$$H^{\mu\nu}_{JA} = -16\pi\alpha_s g_{\rho\sigma} \mathrm{Tr}\left[O^{\rho\mu}_f(\not{p}_2-m_f)\overline{O^{\sigma\nu}_{5f}}(\not{p}_1+m_f)\right],$$

$$H^{\mu\nu}_{AJ} = -16\pi\alpha_s g_{\rho\sigma} \mathrm{Tr}\left[O^{\rho\mu}_{5f}(\not{p}_2-m_f)\overline{O^{\sigma\nu}_f}(\not{p}_1+m_f)\right]; \tag{4.4}$$

where $\alpha_s = g_s^2/4\pi$ and $\overline{O^{\sigma\nu}} = \gamma^o(O^{\sigma\nu})^+\gamma^o$. Neglecting the quark masses (for $s \gg 4m_f^2$) we have

$$O^{\rho\mu}_5 = O^{\rho\mu}\gamma_5, \quad \overline{O^{\sigma\nu}} = O^{\nu\sigma}, \quad \overline{O^{\sigma\nu}_5} = O^{\nu\sigma}\gamma_5, \tag{4.5}$$

implying

$$H^{\mu\nu}_{JJ} = H^{\mu\nu}_{AA}, \quad H^{\mu\nu}_{JA} = H^{\mu\nu}_{AJ}. \tag{4.6}$$

This gives for the hadron tensors $H_r^{\mu\nu}$ defined in (B.2)

$$H_1^{\mu\nu} = H_{JJ}^{\mu\nu}$$

$$H_2^{\mu\nu} = H_3^{\mu\nu} = 0 \tag{4.7}$$

$$H_4^{\mu\nu} = H_{JA}^{\mu\nu} .$$

A straightforward evaluation of the traces then yields

$$H_1^{\mu\nu} = \frac{64\pi\alpha_s}{p_1\cdot p_3\; p_2\cdot p_3}\Big\{-g^{\mu\nu}\left[(p_1\cdot q)^2+(p_2\cdot q)^2\right] - q^2\left(p_1^\mu p_1^\nu + p_2^\mu p_2^\nu\right) + p_1\cdot q\left(p_1^\mu q^\nu + q^\mu p_1^\nu\right) + p_2\cdot q\left(p_2^\mu q^\nu + q^\mu p_2^\nu\right)\Big\},$$

$$H_4^{\mu\nu} = \frac{64\pi\alpha_s}{p_1\cdot p_3\; p_2\cdot p_3}(-i)\,\epsilon^{\mu\nu\rho\sigma}\left[p_1\cdot q\; p_{1\rho} q_\sigma - p_2\cdot q\; p_{2\rho} q_\sigma\right], \tag{4.8}$$

where $\epsilon^{\mu\nu\rho\sigma}$ is the totally antisymmetric tensor with $\epsilon_{o123} = +1$. As discussed in section 2 we need only the space-space components H_r^{mn} in the center of mass system $q^\mu = (Q;\vec{0})$:

$$H_1^{mn} = \frac{64\pi\alpha_s}{(1-x_1)(1-x_2)}\left[(x_1^2+x_2^2)\delta^{mn} - \left(x_1^2\hat{p}_1^m\hat{p}_1^n + x_2^2\hat{p}_2^m\hat{p}_2^n\right)\right],$$

$$H_4^{mn} = \frac{64\pi\alpha_s}{(1-x_1)(1-x_2)}\; i\epsilon^{mnk}\left(x_1^2\hat{p}_1^k - x_2^2\hat{p}_2^k\right). \tag{4.9}$$

Here $x_j = E_j/E_{beam} = 2E_j/Q = 2q\cdot p_j/q^2$ is the scaled energy of parton j and $\hat{p}_j$ is a unit vector along its momentum, i.e. $\vec{p}_j = E_j\,\hat{p}_j = \frac{Q}{2}x_j\,\hat{p}_j$. Energy and momentum conservation imply

$$x_1 + x_2 + x_3 = 2 ,$$

$$x_1\hat{p}_1 + x_2\hat{p}_2 + x_3\hat{p}_3 = 0 , \tag{4.10}$$

so that the events are planar and populate a triangular Dalitz plot in the (x_1, x_2)-plane, for instance.

We now observe that H_1^{mn} is real (symmetric), whereas H_4^{mn} is imaginary (antisymmetric). This means that the quantities ϑ_1 to ϑ_6 (ϑ_7 to ϑ_9) in (B.3) receive contributions only from H_1 (H_4). The same is then true for $\sigma_{\alpha r}^f$ from (2.14), the quantities we actually need. Since the J-factor appearing in (2.14) is

$$J = \left[16\,(2\pi)^2\right]^{-1} \qquad \text{for} \quad d\{x\} = dx_1 dx_2 , \tag{4.11}$$

as can be easily shown by choosing, for instance, Oxyz as indicated in Fig. 3a,b, the cross sections $\sigma_{\alpha r}$ are given by

$$\sigma_{U1} = \frac{2\alpha_s}{\pi}\,\frac{1}{(1-x_1)(1-x_2)}\cdot\frac{1}{2}\left[x_1^2(1+\hat{p}_{1z}^2) + x_2^2(1+\hat{p}_{2z}^2)\right],$$

$$\sigma_{L1} = \text{-"-}\cdot\frac{1}{2}\left[x_1^2(1-\hat{p}_{1z}^2) + x_2^2(1-\hat{p}_{2z}^2)\right],$$

$$\sigma_{T1} = \text{-"-}\cdot\frac{1}{4}\left[x_1^2(\hat{p}_{1x}^2-\hat{p}_{1y}^2) + x_2^2(\hat{p}_{2x}^2-\hat{p}_{2y}^2)\right],$$

$$\sigma_{41} = \text{-"-}\cdot\frac{1}{2}\left[x_1^2\,\hat{p}_{1x}\hat{p}_{1y} + x_2^2\,\hat{p}_{2x}\hat{p}_{2y}\right],$$

$$\sigma_{51} = \text{-"-}\cdot\frac{1}{2\sqrt{2}}\left[x_1^2\,\hat{p}_{1y}\hat{p}_{1z} + x_2^2\,\hat{p}_{2y}\hat{p}_{2z}\right],$$

$$\sigma_{61} = \text{-"-}\cdot\frac{1}{2\sqrt{2}}\left[x_1^2\,\hat{p}_{1z}\hat{p}_{1x} + x_2^2\,\hat{p}_{2z}\hat{p}_{2x}\right],$$

$$\sigma_{\alpha 1} = 0 \quad \text{for} \quad \alpha = 7, 8, 9 ;$$

$$\sigma_{\alpha 2} = \sigma_{\alpha 3} = 0 \quad \text{for} \quad \alpha = 1, 2, \dots, 9 ;$$

$$\sigma_{\alpha 4} = 0 \quad \text{for} \quad \alpha = 1, 2, \dots, 6 ;$$

$$\sigma_{74} = \frac{2\alpha_s}{\pi}\,\frac{1}{(1-x_1)(1-x_2)}\cdot\left[x_1^2\,\hat{p}_{1z} - x_2^2\,\hat{p}_{2z}\right],$$

$$\sigma_{84} = \text{-"-}\cdot\frac{1}{2\sqrt{2}}\left[x_1^2\,\hat{p}_{1x} - x_2^2\,\hat{p}_{2x}\right],$$

$$\sigma_{94} = \text{-"-}\cdot\frac{1}{2\sqrt{2}}\left[x_1^2\,\hat{p}_{1y} - x_2^2\,\hat{p}_{2y}\right]. \tag{4.12}$$

These cross sections actually do not depend on $s = q^2$ and the flavour index f (as a consequence of neglecting m_f). They only depend on the scaled energies x_i as the components $\hat{p}_{jx}$, $\hat{p}_{jy}$ and $\hat{p}_{jz}$ of $\hat{p}_j$ in the body-fixed frame can be expressed through x_i (i.e. given x_i the relative angles between the three jets are determined).

The particularly simple form (4.12) we obtained for $\sigma_{\alpha r}$ is a consequence of our approximations: lowest order QCD (tree-graphs only) and $m_f = 0$. If we let $m_f \neq 0$ in (4.4), then (4.5)-(4.7) no longer hold and we obtain contributions from all H_r, $r = 1, 2, 3, 4$. But since $H_r (r = 1, 2, 3)$ are still real, they only contribute to $\sigma_{\alpha r}$ for $\alpha = 1, 2, \ldots, 6$; the still imaginary H_4 instead contributes only to $\sigma_{\alpha 4}$ for $\alpha = 7, 8, 9$. In higher order QCD (loops) the hadron tensors $H_r (r = 1, 2, 3)$ develop an imaginary part contributing to $\sigma_{\alpha r}$ for $\alpha = 7, 8, 9$; similarly H_4 develops a real part contributing to $\sigma_{\alpha 4}$ for $\alpha = 1, 2, \ldots, 6$. These contributions of "wrong" symmetry can be used, in principle, to test higher order corrections in QCD [2,3]. Contributions of "wrong" symmetry also occur in lowest order QCD if spin effects of the quarks are included [12].

4b) Helicity frame distributions

According to (4.10) the three vectors $\hat{p}_j$ lie in a plane. If this event plane is chosen as the Ozx plane of our body-fixed frame, then $\hat{p}_{jy} = 0$ for $j = 1, 2, 3$ and from (4.12) we find

$$\sigma_{L1} = 2\sigma_{T1} \; ,$$
$$\sigma_{41} = \sigma_{51} = \sigma_{94} = 0 . \qquad (4.13)$$

For the cross sections $S^f_{K\alpha}$ (3.6) we then get

$$S^f_{K\alpha} = \begin{cases} G^f_{K1}\sigma_{\alpha 1} & \text{for } K = A, B, C \text{ and } \alpha = 1,2,3,6 ; \\ G^f_{D4}\sigma_{\alpha 4} & \text{for } K = D \text{ and } \alpha = 7, 8 ; \\ 0 & \text{for all others.} \end{cases} \qquad (4.14)$$

Thus only G^f_{A1}, G^f_{B1}, G^f_{C1} and G^f_{D4} from (2.19) enter the cross sections (2.18), (2.21) - (2.27). These coefficients, however, are the same as those already entering the 2-jet cross section and denoted in [7] by G^f_1, G^f_3, G^f_4 and G^f_5, respectively. Thus, compared with $q\bar{q}$ 2-jet events, no additional information regarding the Z^o can be obtained from the study of $q\bar{q}g$ 3-jet events. In particular, the angular distribution of a momentum-analyzer as given by (2.22) now reads

$$\frac{(2\pi)}{\sigma_{pt}} \frac{d^4\sigma^f}{d\varphi\, d\cos\theta\, dx_1 dx_2} = \frac{3}{8}(\sigma_{U1} + 2\sigma_{L1})\Big\{ G^f_{A1}(1 + \alpha\cos^2\theta) + \alpha G^f_{B1}\sin^2\theta\cos 2\varphi + \alpha G^f_{C1}\sin^2\theta\sin 2\varphi + \epsilon G^f_{D4}\, 2\cos\theta \Big\} , \qquad (4.15)$$

where the flavour independent parameters

$$\alpha = \frac{\sigma_{U1} - 2\sigma_{L1}}{\sigma_{U1} + 2\sigma_{L1}} , \qquad \epsilon = \frac{\sigma_{74}}{\sigma_{U1} + 2\sigma_{L1}} \qquad (4.16)$$

depend on x_1, x_2 and take the effect of the gluon into account (they are identical to the corresponding parameters already used in $q\bar{q}g$-physics in the 1γ-exchange apprixomation). For $\alpha = 1$ and $\epsilon = 1$ the expression inside the bracket in (4.15) reduces to the well-known angular distribution of 2-jet events. The discussion of these events as done in [7] can be overtaken for 3-jet events by simply replacing

$$\begin{aligned} 1 + \cos^2\theta &\longrightarrow 1 + \alpha\cos^2\theta , & G^f_4 &\to \alpha G^f_{C1} , \\ G^f_1 &\longrightarrow \alpha G^f_{A1} , & G^f_5 &\to \epsilon G^f_{D4} . \\ G^f_3 &\longrightarrow \alpha G^f_{B1} , & & \end{aligned} \qquad (4.17)$$

The angular asymmetries of 2-jet events are thus reduced by a factor α or ϵ for 3-jet events due to gluon radiation. Note also that the $(1 + \alpha\cos^2\theta)$-term of the normalized angular distribution does not feel the presence of the Z^o; this shows up only in the φ-dependent terms (with "strength" G^f_{B1}/G^f_{A1} for $\cos 2\varphi$, and G^f_{C1}/G^f_{A1} for $\sin 2\varphi$), or in the $\cos\theta$-term (with "strength" G^f_{D4}/G^f_{A1}). For naturally polarized beams these "strengths" are given by $\mathbf{P}^2 A_{21}^f$, $\mathbf{P}^2 A_{31}^f$ and A_{44}^f respectively, where $A_{r'r}^f$ have been defined in (2.9). These asymmetry parameters are the same as those appearing in the 2-jet distributions and denoted in [7] by A_3^f, A_4^f and A_5^f respectively. Their energy dependence is shown in Figs. 4, 5 and 6 for different flavours and within the Weinberg-Salam model, see Table I. In this model the mass of the Z^o is given by

$$M_Z \sqrt{g} = (2 \sin 2\theta_W)^{-1} , \tag{4.18}$$

where g is the same coupling constant as in (2.1). The total width Γ_Z is assumed to be given by the decays $Z^o \rightarrow f\bar{f}$ into all pairs of fundamental fermions much lighter than the Z^o ($2m_f \ll M_Z$), i.e.

$$\Gamma_Z \approx \frac{G_F M_Z^3}{24 \pi \sqrt{2}} \sum_{f=\nu,\ell,u,d} (v_f^2 + a_f^2) . \tag{4.19}$$

Here the sum goes over all N_f kinds of neutrinos (N_ν), charged leptons (N_ℓ), up-quarks (N_u) and down-quarks (N_d), each quark flavour coming in three colours. In our numerical calculation we have assumed $N_\nu = N_\ell = N_u = N_d = 3$ and $\sin^2\theta_W = 0.23$, yielding $M_Z = 89$ GeV and $\Gamma_Z = 2.5$ GeV. The resulting asymmetry parameters A_{21}^f (Fig.4) and A_{44}^f (Fig.6) show a quite remarkable energy dependence which should be manifest in the angular distribution even much below the Z^o-pole, especially for d-quarks. The parameter A_{31}^f (Fig.5) instead remains unobservably small (less than 4%) over the whole energy range.

Regarding the θ,χ-distribution (2.26) we get $\alpha_4^f = \alpha_5^f = \epsilon_9^f = 0$ from (2.27) and (4.14), and thus

$$\frac{(2\pi)}{\sigma_{pt}} \frac{d^4\sigma^f}{d\cos\theta \, d\chi \, dx_1 dx_2} = \frac{3}{8}(\sigma_{U1} + 2\sigma_{L1}) G_{A1}^f \Big\{ 1 + \alpha \cos^2\theta$$

$$+ \alpha_T \sin^2\theta \cos 2\chi + \alpha_I \sin 2\theta \cos\chi$$

$$+ (G_{D4}^f / G_{A1}^f)(2\epsilon \cos\theta + \epsilon_8 \sin\theta \cos\chi) \Big\} , \tag{4.20}$$

with α and ϵ from (4.16) and (index U,L,T,I for $\alpha = 1,2,3,6$)

$$\alpha_T = 2\sigma_{T1} / (\sigma_{U1} + 2\sigma_{L1}) = (1-\alpha)/4 ,$$

$$\alpha_I = -2\sqrt{2}\, \sigma_{I1} / (\sigma_{U1} + 2\sigma_{L1}) ,$$

$$\epsilon_8 = -4\sqrt{2}\, \sigma_{84} / (\sigma_{U1} + 2\sigma_{L1}) . \tag{4.21}$$

Apart from a normalization factor G_{A1}^f, the Z^o shows up only in the ϵ-terms with "strength" G_{D4}^f/G_{A1}^f. The angle-integrated cross section follows from (2.25), (4.14) and (4.12):

$$\frac{1}{\sigma_{pt}} \frac{d^2\sigma^f}{dx_1 dx_2} = G_{A1}^f \frac{2\alpha_s}{\pi} \frac{x_1^2 + x_2^2}{(1-x_1)(1-x_2)} . \tag{4.22}$$

Thus the Z^o has no influence on the x_1, x_2-distribution, but only on the event rate.

Up to now we have not really fixed our helicity frame to the final state. This must be done, however, since otherwise the angles φ, θ, χ cannot be determined unambiguously. As it is not possible yet to say which of the three observed jets is the quark, antiquark or gluon jet, we have to rely on energy ordering. We denote by $T_1 = T = \max(x_1, x_2, x_3)$ the scaled energy of the most energetic jet and by T_2 that of the second most energetic jet. Then $T_3 = 2 - T_1 - T_2$ is the scaled energy of the least energetic jet and we have the kinematical limits

$$\frac{2}{3} \leq T \leq 1 , \qquad (1 - \tfrac{1}{2}T) \leq T_2 \leq T ,$$

$$2(1-T) \leq T_3 \leq (1 - \tfrac{1}{2}T) . \tag{4.23}$$

If $\hat{T}_1$, $\hat{T}_2$ and $\hat{T}_3$ are unit vectors pointing into the direction of the corresponding jets, then the angles $\theta_{ij} \in [0,\pi]$ between these jets are defined through

$$c_{ij} = \cos\theta_{ij} = \hat{T}_i \cdot \hat{T}_j = 1 - 2(T_i + T_j - 1)/T_i T_j ,$$

$$s_{ij} = \sin\theta_{ij} = 2\sqrt{(1-T_1)(1-T_2)(1-T_3)} \,/\, T_i T_j . \tag{4.24}$$

We now choose the body-fixed frame as shown in Fig.3a, b: Oz along $\hat{T}_1$ and Ox in the event plane such that $\hat{T}_2 \cdot \hat{x} > 0$. We refer to this choice as the thrust frame. According to which parton is most (second most) energetic, we distinguish six regions j_i (for $x_j = T_1$, $x_i = T_2$) of the Dalitz plot;

$$
\begin{aligned}
1_2:\ & x_1 = T_1\quad x_2 = T_2,\quad x_3 = 2-T_1-T_2 ,\\
& \hat{p}_1 = (0, 0, 1) ,\\
& \hat{p}_2 = (s_{12}, 0, c_{12}) ;\\[2mm]
1_3:\ & x_1 = T_1,\ x_2 = 2-T_1-T_2,\quad x_3 = T_2 ,\\
& \hat{p}_1 = (0, 0, 1) ,\\
& \hat{p}_2 = (-s_{13}, 0, c_{13}) ;\\[2mm]
2_1:\ & x_1 = T_2,\ x_2 = T_1,\ x_3 = 2-T_1-T_2 ,\\
& \hat{p}_1 = (s_{12}, 0\ c_{12}) ,\\
& \hat{p}_2 = (0, 0, 1) ;\\[2mm]
2_3:\ & x_1 = 2-T_1-T_2,\quad x_2 = T_1,\quad x_3 = T_2 ,\\
& \hat{p}_1 = (-s_{13}, 0, c_{13}) ,\\
& \hat{p}_2 = (0, 0, 1) ;\\[2mm]
3_1:\ & x_1 = T_2,\quad x_2 = 2-T_1-T_2,\quad x_3 = T_1 ,\\
& \hat{p}_1 = (s_{12}, 0, c_{12}) ,\\
& \hat{p}_2 = (-s_{13}, 0, c_{13}) ;\\[2mm]
3_2:\ & x_1 = 2-T_1-T_2,\quad x_2 = T_2,\quad x_3 = T_1 ,\\
& \hat{p}_1 = (-s_{13}, 0, c_{13}) ,\\
& \hat{p}_2 = (s_{12}, 0, c_{12}) .
\end{aligned}
\tag{4.25}
$$

Using these expressions for x_i and $\hat{p}_i$ in (4.12) we get the cross sections $(\sigma_{\alpha r})_{j_i} = (d^2\sigma_{\alpha r}/dT_1 dT_2)_{j_i}$ in the respective regions of the Dalitz plot. Integrating over T_2 we find $(d\sigma_{\alpha r}/dT)_{j_i}$ as a function of thrust T. The thrust distributions themselves are then given by

$$
d\sigma_{\alpha r}/dT = \sum_k \left(d\sigma_{\alpha r}/dT \right)_k \tag{4.26}
$$

where the sum is taken over $k = 1_2,\ 1_3,\ 2_1,\ 2_3,\ 3_1$ and 3_2. It follows from (4.25) and (4.12) that there is no constribution to $d\sigma_{\alpha r}/dT$ for

$\alpha = 7, 8, 9$. In this case the ϵ-terms in (4.15) and (4.20) vanish and the only way to see the Z^o in the angular distribution of the thrust axis is through G^f_{B1}/G^f_{A1} and G^f_{C1}/G^f_{A1} in (4.15) for transversely polarized beams.

In order to get nonvanishing contributions to the cross sections $\sigma_{\alpha r}$ (for $\alpha = 7, 8, 9$) which are odd under $q \leftrightarrow \bar{q}$, we have to consider distributions to which q and $\bar{q}$ contribute differently. One possibility is to study semi-inclusive hadron production, i.e. to weight quarks and antiquarks by their fragmentation functions D^h_q and $D^h_{\bar{q}}$ into the same hadron h. This leaves a finite effect due to $D^h_q \neq D^h_{\bar{q}}$ for $h \neq \bar{h}$. The cross sections $S^f_{K\alpha}$ (4.14) have to be replaced now by the cross sections $d^2S^h_{K\alpha}/dT\,dz$ for finding a hadron h along the thrust axis, i.e. arising from the most energetic parton, with fractional momentum $z = x_h/T$. We find

$$
\begin{aligned}
\frac{d^2(S^h_{KU}+S^h_{KL})}{dT\,dz} &= \frac{2\alpha_s}{\pi}\sum_f G^f_{K1}\Big\{\Big[-\frac{(4-T)(3T-2)}{2(1-T)} + \frac{1+T^2}{1-T}\ln\Big(\frac{2T-1}{1-T}\Big)\Big]\Big(D^h_{q_f}(z)+D^h_{\bar{q}_f}(z)\Big)\\
&\qquad + \Big[-2(3T-2)+\frac{2}{T}(2-2T+T^2)\ln\Big(\frac{2T-1}{1-T}\Big)\Big]D^h_g(z)\Big\} ,\\
\frac{d^2S^h_{KL}}{dT\,dz} &= \frac{2\alpha_s}{\pi}\sum_f G^f_{K1}\ \frac{(3T-2)}{T}\Big[\Big(D^h_{q_f}(z)+D^h_{\bar{q}_f}(z)\Big) + \frac{4}{T}(1-T)\,D^h_g(z)\Big] ,\\
\frac{d^2S^h_{KT}}{dT\,dz} &= \frac{1}{2}\ \frac{d^2S^h_{KL}}{dT\,dz} ,\\
\frac{d^2S^h_{KI}}{dT\,dz} &= \frac{2\alpha_s}{\pi}\sum_f G^f_{K1}\ \frac{1}{\sqrt{2}}\Big(\frac{2}{T}\sqrt{2T-1}-\frac{1}{\sqrt{1-T}}\Big)\Big[\Big(D^h_{q_f}(z)+D^h_{\bar{q}_f}(z)\Big)+\frac{2}{T}(1-T)(2-T)\,D^h_g(z)\Big] ;\\[3mm]
\frac{d^2S^h_{D7}}{dT\,dz} &= \frac{2\alpha_s}{\pi}\sum_f G^f_{D4}\Big[-\frac{(4-2T+T^2)(3T-2)}{2T\,(1-T)} + \frac{1+T^2}{1-T}\ln\Big(\frac{2T-1}{1-T}\Big)\Big]\Big(D^h_{q_f}(z)-D^h_{\bar{q}_f}(z)\Big) ,\\
\frac{d^2S^h_{D8}}{dT\,dz} &= \frac{2\alpha_s}{\pi}\sum_f G^f_{D4}\ \frac{1}{\sqrt{2}}\Big(\frac{2}{T}\sqrt{2T-1}-\frac{1}{\sqrt{1-T}}\Big)\Big(D^h_{q_f}(z)-D^h_{\bar{q}_f}(z)\Big) .
\end{aligned}
\tag{4.27}
$$

Here K = A, B, C; all other cross sections vanish. Disregarding the factors G^f_{K1} and G^f_{D4}, the coefficients multiplying $D^h_{q_f}$, $D^h_{\bar{q}_f}$ and D^h_g are nothing else than the well-known jet cross sections associated, respectively, with the quark, antiquark and gluon forming the thrust and where the momenta of the recoiling less energetic partons have been integrated out. In the notation of (4.26) they are given, respectively, by $(d\sigma_{\alpha r}/dT)_{1_2+1_3}$, $(d\sigma_{\alpha r}/dT)_{2_1+2_3}$ and $(d\sigma_{\alpha r}/dT)_{3_1+3_2}$. As expected, there is no contribution of the flavourless gluon to the charge asymmetric cross sections S^h_{D7} and S^h_{D8} (remember $D^h_{\bar{q}} = D^{\bar{h}}_q$ by charge conjugation). The thrust cross sections $dS_{K\alpha}/dT$ can be obtained from (4.26) by integrating over z and summing over all hadrons h. Formally this amounts to replacing all fragmentation functions by 1. One then recovers $dS_{D7}/dT = dS_{D8}/dT = 0$.

We now want to examine the effect of higher order QCD corrections for the final state in (4.1). In lowest order we found H^{mn}_1 = real, H^{mn}_4 = imaginary, and $H^{mn}_2 = H^{mn}_3 = 0$, see (4.7) - (4.9). This led to (4.12) with $H_1 (H_4)$ contributing only to $\sigma_{\alpha 1} (\sigma_{\alpha 4})$ for $\alpha = 1 \div 6$ ($\alpha = 7 \div 9$). Suppose now that in higher order QCD, due to loop integrals, H^{mn}_1 (H^{mn}_4) develops an imaginary (real) part. Then we get contributions to $\sigma_{\alpha 1} (\sigma_{\alpha 4})$ also for $\alpha = 7 \div 9$ ($\alpha = 1 \div 6$). How would these contributions of "wrong" symmetry show up in the angular distribution? Since the events are still planar we can use (3.6) to obtain the following additional cross sections (compared with (4.14)):

$$S^f_{K\alpha} = G^f_{K4}\, \sigma_{\alpha 4} \qquad K = A, B, C \quad \text{and} \quad \alpha = 4, 5,$$
$$S^f_{D9} = G^f_{D1}\, \sigma_{91} . \tag{4.28}$$

The corresponding angular coefficients can be read off from (2.21). In particular, the distribution (4.15) remains unchanged, whereas (4.20) gets modified by

$$\frac{3}{8}\Big\{ G^f_{A4} \left(-2\sigma_{44} \sin^2\theta \sin 2\chi + 2\sqrt{2}\, \sigma_{54} \sin 2\theta \sin\chi \right) + G^f_{D1} \left(4\sqrt{2}\, \sigma_{91} \sin\theta \sin\chi \right) \Big\} . \tag{4.29}$$

The new cross sections appear with Z^0-related "strengths" given by G^f_{Kr}/G^f_{A1}. The latter reduce for naturally polarized beams to A^f_{14}, $P^2 A^f_{24}$, $P^2 A^f_{34}$ and A^f_{41}, where $A^f_{r'r}$ is defined in (2.7). The energy dependence of these parameters is shown in Fig.7 to 10, again in the Weinberg-Salam model and for $\sin^2\theta_W = 0.23$.

4c) Transversity-frame distributions

We now choose the event plane as the Oxy-plane of our body-fixed frame so that $\hat{p}_{jz} = 0$ for j = 1, 2, 3. From (4.12) we then get

$$\bar{\sigma}_{U1} = \bar{\sigma}_{L1} ,$$
$$\bar{\sigma}_{51} = \bar{\sigma}_{61} = \bar{\sigma}_{74} = 0 , \tag{4.30}$$

and from (3.13)

$$\bar{S}^f_{K\alpha} = \begin{cases} G^f_{K1}\, \bar{\sigma}_{\alpha 1} & \text{for } K = A, B, C \text{ and } \alpha = 1,2,3,4 ; \\ G^f_{D4}\, \bar{\sigma}_{\alpha 4} & \text{for } K = D \text{ and } \alpha = 8,9 ; \\ 0 & \text{for all others.} \end{cases} \tag{4.31}$$

These relations also follow from (3.15) and (4.13), (4.14). The general angular distribution is then given by (2.21) with φ, θ, χ and $S^f_{K\alpha}$ replaced simply by $\bar{\varphi}, \bar{\theta}, \bar{\chi}$ and $\bar{S}^f_{K\alpha}$. Thus the angular distribution of the normal to the event plane would be given by (2.22) or, equivalently, by (4.15), but in terms of the bared quantities refering to the transversity frame, i.e.

$$\frac{(2\pi)}{\sigma_{pt}}\,\frac{d^4\bar\sigma^f}{d\bar\varphi\,d\cos\bar\theta\,dx_1dx_2} = \frac{3}{8}(\bar\sigma_{U1}+2\bar\sigma_{L1})\Big\{G^f_{A1}(1+\bar\alpha\cos^2\bar\theta)$$
$$+\bar\alpha\,G^f_{B1}\sin^2\bar\theta\cos 2\bar\varphi + \bar\alpha\,G^f_{C1}\sin^2\bar\theta\sin 2\bar\varphi + \bar\epsilon\,G^f_{D4}\,2\cos\bar\theta\Big\}. \tag{4.32}$$

Here $\bar\alpha$ and $\bar\epsilon$ are defined as in (4.16), but in terms of $\bar\sigma_{\alpha r}$, i.e.

$$\bar\alpha = (\bar\sigma_{U1}-2\bar\sigma_{L1})/(\bar\sigma_{U1}+2\bar\sigma_{L1}) = -1/3\ ,$$
$$\bar\epsilon = \bar\sigma_{74}/(\bar\sigma_{U1}+2\bar\sigma_{L1}) = 0, \tag{4.33}$$

where (4.30) has been used for the last equalities. This gives the well-known $(1-\frac{1}{3}\cos^2\theta) = \frac{1}{3}(2+\sin^2\theta)$ distribution of the normal to the event plane. Note also that the whole dependence on x_1, x_2 is contained in the overall factor $(\bar\sigma_{U1}+2\bar\sigma_{L1}) = 3\bar\sigma_{U1}$.

The $\bar\theta$, $\bar\chi$-distribution follows from (2.26), (2.27) and (4.31):

$$\frac{(2\pi)}{\sigma_{pt}}\,\frac{d^4\bar\sigma^f}{d\cos\bar\theta\,d\bar\chi\,dx_1dx_2} = \frac{3}{8}(\bar\sigma_{U1}+2\bar\sigma_{L1})\,G^f_{A1}\Big\{(1-\tfrac{1}{3}\cos^2\bar\theta)$$
$$+\bar\alpha_T\sin^2\bar\theta\cos 2\bar\chi + \bar\alpha_I\sin^2\bar\theta\sin 2\bar\chi$$
$$+(G^f_{D4}/G^f_{A1})(\bar\epsilon_8\sin\bar\theta\cos\bar\chi + \bar\epsilon_9\sin\bar\theta\sin\bar\chi)\Big\}, \tag{4.34}$$

where now (index U,L,T,I for $\alpha = 1,2,3,4$)

$$\bar\alpha_T = (2/3)\,\bar\sigma_{T1}/\bar\sigma_{U1}\ ,\qquad \bar\alpha_I = (-2/3)\,\bar\sigma_{I1}/\bar\sigma_{U1}\ ,$$
$$\bar\epsilon_8 = (-4\sqrt{2}/3)\,\bar\sigma_{84}/\bar\sigma_{U1}\ ,\qquad \bar\epsilon_9 = (4\sqrt{2}/3)\,\bar\sigma_{94}/\bar\sigma_{U1}\ . \tag{4.35}$$

The angle-integrated cross section is given by (4.22) again.

If the distributions are analyzed in terms of thrust, a possible choice of the transversity frame would be (compare Fig.3c): Ox along $\hat T_1$ and Oz along $\hat T_1 \times \hat T_2$. Then the cross sections $(d^2\bar\sigma_{\alpha r}/dT_1dT_2)_{j_i}$

refering to the region j_i of the Dalitz plot can be obtained from (4.12) by using the components of $\hat p_i$ in the frame just defined. For example, in region 1_2 we now have instead of (4.25): $\hat p_1 = (1, 0, 0)$, $\hat p_2 = (c_{12}, s_{12}, 0)$, and similarly for the other regions. But instead of doing so it is much simpler to obtain $\bar\sigma_{\alpha r}$ from the helicity-frame quantities $\sigma_{\alpha r}$ given in the previous subsection by using (3.15). From (4.27) we then obtain

$$\frac{d^2\bar S^h_{KU}}{dT\,dz} = \frac{2\alpha_s}{\pi}\sum_f G^f_{K1}\Big\{\Big[-\frac{(4-T)(3T-2)}{4(1-T)} + \frac{1+T^2}{2(1-T)}\ln\Big(\frac{2T-1}{1-T}\Big)\Big]\Big(D^h_{q_f}(z)+D^h_{\bar q_f}(z)\Big)$$
$$+\Big[-(3T-2)+\frac{1}{T}(2-2T+T^2)\ln\Big(\frac{2T-1}{1-T}\Big)\Big]D^h_g(z)\Big\}\ ,$$

$$\frac{d^2\bar S^h_{KL}}{dT\,dz} = \frac{d^2\bar S^h_{KU}}{dT\,dz}\ ,$$

$$\frac{d^2\bar S^h_{KT}}{dT\,dz} = \frac{2\alpha_s}{\pi}\sum_f G^f_{K1}\Big\{\Big[-\frac{(8-4T-T^2)(3T-2)}{8T(1-T)} + \frac{1+T^2}{4(1-T)}\ln\Big(\frac{2T-1}{1-T}\Big)\Big]\Big(D^h_{q_f}(z)+D^h_{\bar q_f}(z)\Big)$$
$$+\frac{1}{2T^2}\Big[-(8-8T+T^2)(3T-2)+T(2-2T+T^2)\ln\Big(\frac{2T-1}{1-T}\Big)\Big]D^h_g(z)\Big\},$$

$$\frac{d^2\bar S^h_{KI}}{dT\,dz} = \frac{2\alpha_s}{\pi}\sum_f G^f_{K1}\Big(\frac{2}{T}\sqrt{2T-1}-\frac{1}{\sqrt{1-T}}\Big)\Big[\Big(D^h_{q_f}(z)+D^h_{\bar q_f}(z)\Big)+\frac{2}{T}(1-T)(2-T)D^h_g(z)\Big]\ ;$$

$$\frac{d^2\bar S^h_{D8}}{dT\,dz} = \frac{2\alpha_s}{\pi}\sum_f G^f_{D4}\frac{1}{2\sqrt{2}}\Big[-\frac{(4-2T+T^2)(3T-2)}{2T(1-T)} + \frac{1+T^2}{1-T}\ln\Big(\frac{2T-1}{1-T}\Big)\Big]\Big(D^h_{q_f}(z)-D^h_{\bar q_f}(z)\Big),$$

$$\frac{d^2\bar S^h_{D9}}{dT\,dz} = \frac{2\alpha_s}{\pi}\sum_f G^f_{D4}\frac{1}{\sqrt{2}}\Big(\frac{2}{T}\sqrt{2T-1}-\frac{1}{\sqrt{1-T}}\Big)\Big(D^h_{q_f}(z)-D^h_{\bar q_f}(z)\Big)\ , \tag{4.36}$$

where K = A, B, C and all other cross sections vanish. The angular distribution is then given by (2.21) with φ, θ, χ and $S^f_{K\alpha}$ replaced by $\bar\varphi$, $\bar\theta$, $\bar\chi$ and $d\bar S^h_{K\alpha}/dT\,dz$. Regarding the charge asymmetric cross sections $\bar S^h_{D8}$ and $\bar S^h_{D9}$ the same discussion applies as for S^h_{D7} and S^h_{D8} in subsection 4b .

Finally we are looking for higher order QCD corrections resulting in an imaginary (real) part of H^{mn}_1 (H^{mn}_4). From (3.13) we obtain the following additional cross sections (compared with (4.31)):

$$\bar S^f_{K\alpha} = G^f_{K4}\,\bar\sigma_{\alpha 4} \qquad \text{for } K = A,B,C \text{ and } \alpha = 5,6\ ,$$
$$\bar S^f_{D7} = G^f_{D1}\,\bar\sigma_{71}\ . \tag{4.37}$$

Here the same G^f_{K4} and G^f_{D1} as in (4.28) appear, but with different angular coefficients as can be read off from (2.21). In particular, the distribution (4.32) gets modified by

$$\frac{3}{8}\left\{ G^f_{D1}\,\bar{\sigma}_{71}\; 2\cos\bar{\theta} \right\}, \tag{4.38}$$

and the distribution (4.34) by

$$\frac{3}{8}\left\{ G^f_{A4}\; 2\sqrt{2}\left[\bar{\sigma}_{54}\sin 2\bar{\theta}\sin\bar{\chi} - \bar{\sigma}_{64}\sin 2\bar{\theta}\cos\bar{\chi} \right] + G^f_{D1}\,\bar{\sigma}_{71}\; 2\cos\bar{\theta} \right\}. \tag{4.39}$$

Thus there appears a foward-backward asymmetry of the normal to the event plane which directly measures higher order QCD effects [2,3] with "strength" G^f_{D1}/G^f_{A1}, i.e. A^f_{41} for unpolarized beams (see Fig.10). For $Q_f=-1/3$ A^f_{41} is quite large already at the upper PETRA and PEP energies.

5. Concluding Remarks

The zeroth order cross sections can be obtained from (4.27) and (4.36) by multiplication with

$$\left[\frac{8}{3}\,\frac{\alpha_s}{\pi}\; \frac{|\ln(1-T)|}{1-T} \right]^{-1} \tag{5.1}$$

and taking the limit $T \to 1$. The result is

$$\frac{d(S^h_{KU}+S^h_{KL})}{dx_h} = \frac{d(\bar{S}^h_{KU}+\bar{S}^h_{KL})}{dx_h} = \frac{3}{2}\sum_f G^f_{K1}\left(D^h_{q_f}(x_h)+D^h_{\bar{q}_f}(x_h)\right),$$

$$\frac{d S^h_{D7}}{dx_h} = \frac{3}{2}\sum_f G^f_{D4}\left(D^h_{q_f}(x_h)-D^h_{\bar{q}_f}(x_h)\right),$$

$$\frac{d \bar{S}^h_{D8}}{dx_h} = \frac{3}{4\sqrt{2}}\sum_f G^f_{D4}\left(D^h_{q_f}(x_h)-D^h_{\bar{q}_f}(x_h)\right), \tag{5.2}$$

while all other cross sections are zero (cf. Ref.[7]).

The list of cross sections given in section 4 is incomplete inasmuch as the quark masses have been set to zero. The extension to massive quarks (including the calculation of the extra cross sections) is now straightforward but still has to be done. It is probably only for the heavy quarks that one can detect the forward-backward asymmetry since this requires to be able to distinguish between quarks and antiquarks. For the heavy quarks this should be relatively easy because of their weak decays.

Appendix A: The lepton tensor

In this appendix we consider the various lepton tensors associated with the vertices $e^-e^+ \to \gamma$ and $e^-e^+ \to Z^0$. We use the metric tensor $g^{\mu\nu} = g_{\mu\nu} = \mathrm{diag}\,(1; -1, -1, -1)$ and the conventions of Bjorken and Drell [13].

The lepton tensors $L_r^{\mu\nu}$, $r = 1, \ldots, 4$, appearing in (2.6) are defined in terms of

$$
\begin{aligned}
L^{\mu\nu}_{jj} &= (2s)^{-1}\, \mathrm{Tr}\left(\gamma^\mu \rho_- \gamma^\nu \rho_+\right), \\
L^{\mu\nu}_{ja} &= (2s)^{-1}\, \mathrm{Tr}\left(\gamma^\mu \rho_- \gamma^\nu \gamma_5 \rho_+\right), \\
L^{\mu\nu}_{aj} &= (2s)^{-1}\, \mathrm{Tr}\left(\gamma^\mu \gamma_5 \rho_- \gamma^\nu \rho_+\right), \\
L^{\mu\nu}_{aa} &= (2s)^{-1}\, \mathrm{Tr}\left(\gamma^\mu \gamma_5 \rho_- \gamma^\nu \gamma_5 \rho_+\right)
\end{aligned}
\tag{A.1}
$$

by the (hermitian) combinations

$$
\begin{aligned}
L^{\mu\nu}_1 &= \tfrac{1}{2}\left(L^{\mu\nu}_{jj} + L^{\mu\nu}_{aa}\right), \\
L^{\mu\nu}_2 &= \tfrac{1}{2}\left(L^{\mu\nu}_{jj} - L^{\mu\nu}_{aa}\right), \\
L^{\mu\nu}_3 &= \tfrac{i}{2}\left(L^{\mu\nu}_{ja} - L^{\mu\nu}_{aj}\right), \\
L^{\mu\nu}_4 &= \tfrac{1}{2}\left(L^{\mu\nu}_{ja} + L^{\mu\nu}_{aj}\right).
\end{aligned}
\tag{A.2}
$$

Here $\rho_\pm$ are given by

$$
\rho_\pm = \left(\not{p}_\pm \mp m_e\right)\left(1 + \gamma_5 \not{s}_\pm\right), \tag{A.3}
$$

where $p_\pm^\mu$ and $s_\pm^\mu$ are the momentum and polarization four-vectors of $e^\pm$ satisfying $p_\pm \cdot p_\pm = m_e^2$, $p_\pm \cdot s_\pm = 0$ and $s_\pm \cdot s_\pm = -|\vec{\xi}^\pm|^2 \geq -1$, $\vec{\xi}^\pm$ being the rest-frame polarization vectors. In the high-energy

limit $s = (p_- + p_+)^2 \gg 4m_e^2$ the expressions (A.3) reduce to

$$
\rho_\pm = \not{p}_\pm \left(1 - \gamma_5\, \vec{\gamma} \cdot \vec{\xi}^\pm_\perp \pm h^\pm \gamma_5\right), \tag{A.4}
$$

where we have introduced the longitudinal (h) and transverse ($\vec{\xi}_\perp$) components of $\vec{\xi}$ with respect to $\hat{p} = \vec{p}/|\vec{p}|$:

$$
h^\pm = \vec{\xi}^\pm \cdot \hat{p}_\pm \,, \qquad \vec{\xi}^\pm_\perp = \vec{\xi}^\pm - h^\pm \hat{p}_\pm \,. \tag{A.5}
$$

We now evaluate the lepton tensors in the center of mass frame Ox'y'z' of Fig. 2, with Oz' along $\hat{p}_-$ and $\vec{p}_- + \vec{p}_+ = 0$. In this frame $h^\pm = \mp \xi^\pm_{z'}$ and $\vec{\xi}^\pm_\perp = (\xi^\pm_{x'}, \xi^\pm_{y'}, 0)$. Using (A.4) in (A.1) and neglecting terms of order $4m_e^2/s$, the only surviving components of $L'^{\mu\nu} = L^{\mu\nu}(\mathrm{Ox'y'z'})$ are those for $\mu, \nu = 1,2$ given by

$$
\begin{aligned}
L_1'^{11} &= L_1'^{22} = (1 - h^- h^+), \\
L_1'^{12} &= -L_1'^{21} = -i(h^- - h^+); \\
L_2'^{11} &= -L_2'^{22} = -\left(\xi^-_{x'}\xi^+_{x'} - \xi^-_{y'}\xi^+_{y'}\right), \\
L_2'^{12} &= L_2'^{21} = -\left(\xi^-_{x'}\xi^+_{y'} + \xi^-_{y'}\xi^+_{x'}\right); \\
L_3'^{11} &= -L_3'^{22} = \left(\xi^-_{x'}\xi^+_{y'} + \xi^-_{y'}\xi^+_{x'}\right), \\
L_3'^{12} &= L_3'^{21} = -\left(\xi^-_{x'}\xi^+_{x'} - \xi^-_{y'}\xi^+_{y'}\right); \\
L_4'^{11} &= L_4'^{22} = (h^- - h^+) \\
L_4'^{12} &= -L_4'^{21} = -i(1 - h^- h^+).
\end{aligned}
\tag{A.6}
$$

Thus longitudinal (transverse) beam polarization contributes only to L_1, L_4 (L_2, L_3); this makes the definitions (A.2) advantageous.

The components L'^{mn} of the lepton tensors in (A.6) refer to the "space-fixed" frame Ox'y'z' of Fig.2. Actually we need the components L^{mn} in the "body-fixed" frame Oxyz. Since Oxyz is obtained from Ox'y'z' by a rotation $R = R(\varphi, \theta, \chi)$ through Euler angles φ, θ and χ, i.e.

$$R = \begin{pmatrix} \cos\varphi\cos\theta\cos\chi - \sin\varphi\sin\chi & -\cos\varphi\cos\theta\sin\chi - \sin\varphi\cos\chi & \sin\theta\cos\varphi \\ \sin\varphi\cos\theta\cos\chi + \cos\varphi\sin\chi & -\sin\varphi\cos\theta\sin\chi + \cos\varphi\cos\chi & \sin\theta\sin\varphi \\ -\sin\theta\cos\chi & \sin\theta\sin\chi & \cos\theta \end{pmatrix} \tag{A.7}$$

we get from the transformation law of a tensor

$$L^{mn}(\varphi,\theta,\chi) = R^{km}(\varphi,\theta,\chi)\, R^{ln}(\varphi,\theta,\chi)\, L'^{kl} \quad , \quad m,n = 1,2,3. \tag{A.8}$$

Although the L'^{kl}'s from (A.6) are of particular form, the resulting expressions for L^{mn} are rather lengthy. Instead of writing them down, we directly give the more compact expressions for the contraction of L^{mn} with an arbitrary tensor H_{mn}:

$$\begin{aligned} L^{mn}H_{mn} &= \tfrac{1}{2}(L^{11}+L^{22})(H_{11}+H_{22}) + \tfrac{1}{2}(L^{11}-L^{22})(H_{11}-H_{22}) + L^{33}H_{33} \\ &+ \left[\tfrac{1}{2}(L^{12}+L^{21})(H_{12}+H_{21}) + \tfrac{1}{2}(L^{12}-L^{21})(H_{12}-H_{21})\right] \\ &+ [2,3] + [3,1]\,. \end{aligned} \tag{A.9}$$

Introducing here $\vartheta_\alpha(H)$ from (B.3) and defining the quantities $\vartheta_K(H)$, K = A, B, C, D by

$$\begin{aligned} \hat\sigma_A &= \tfrac{3}{8}(1+\cos^2\theta)\,\hat\sigma_U + \tfrac{3}{4}\sin^2\theta\,\hat\sigma_L + \tfrac{3}{4}\sin^2\theta\cos 2\chi\,\hat\sigma_T \\ &\quad - \tfrac{3}{4}\sin^2\theta\sin 2\chi\,\hat\sigma_4 + \tfrac{3}{2\sqrt2}\sin 2\theta\sin\chi\,\hat\sigma_5 - \tfrac{3}{2\sqrt2}\sin 2\theta\cos\chi\,\hat\sigma_6\,, \\ \hat\sigma_B &= \tfrac{3}{8}\sin^2\theta\,\hat\sigma_U - \tfrac{3}{4}\sin^2\theta\,\hat\sigma_L + \tfrac{3}{4}(1+\cos^2\theta)\cos 2\chi\,\hat\sigma_T \\ &\quad - \tfrac{3}{4}(1+\cos^2\theta)\sin 2\chi\,\hat\sigma_4 - \tfrac{3}{2\sqrt2}\sin 2\theta\sin\chi\,\hat\sigma_5 + \tfrac{3}{2\sqrt2}\sin 2\theta\cos\chi\,\hat\sigma_6\,, \\ \hat\sigma_C &= \tfrac{3}{2}\cos\theta\sin 2\chi\,\hat\sigma_T + \tfrac{3}{2}\cos\theta\cos 2\chi\,\hat\sigma_4 \\ &\quad + \tfrac{3}{\sqrt2}\sin\theta\cos\chi\,\hat\sigma_5 + \tfrac{3}{\sqrt2}\sin\theta\sin\chi\,\hat\sigma_6\,, \\ \hat\sigma_D &= \tfrac{3}{4}\cos\theta\,\hat\sigma_7 - \tfrac{3}{\sqrt2}\sin\theta\cos\chi\,\hat\sigma_8 + \tfrac{3}{\sqrt2}\sin\theta\sin\chi\,\hat\sigma_9\,, \end{aligned} \tag{A.10}$$

we obtain the following results

$$\begin{aligned} \tfrac{3}{4} L_1^{mn} H_{mn} &= (1-h^-h^+)\,\hat\sigma_A + (h^- - h^+)\,\hat\sigma_D\,, \\ \tfrac{3}{4} L_2^{mn} H_{mn} &= X(\varphi)\,\hat\sigma_B + Y(\varphi)\,\hat\sigma_C\,, \\ \tfrac{3}{4} L_3^{mn} H_{mn} &= X(\varphi)\,\hat\sigma_C - Y(\varphi)\,\hat\sigma_B\,, \\ \tfrac{3}{4} L_4^{mn} H_{mn} &= (1-h^-h^+)\,\hat\sigma_D + (h^- - h^+)\,\hat\sigma_A\,, \end{aligned} \tag{A.11}$$

where

$$\begin{aligned} X(\varphi) &= (\xi^-_{x'}\xi^+_{x'} - \xi^-_{y'}\xi^+_{y'})\cos 2\varphi + (\xi^-_{x'}\xi^+_{y'} + \xi^-_{y'}\xi^+_{x'})\sin 2\varphi\,, \\ Y(\varphi) &= -(\xi^-_{x'}\xi^+_{x'} - \xi^-_{y'}\xi^+_{y'})\sin 2\varphi + (\xi^-_{x'}\xi^+_{y'} + \xi^-_{y'}\xi^+_{x'})\cos 2\varphi\,. \end{aligned} \tag{A.12}$$

For beams of helicity $\lambda^\pm$ ($\lambda^+ = \pm 1/2$, $\lambda^- = \pm 1/2$) we have $h^\pm = 2\lambda^\pm$ and $X(\varphi) = Y(\varphi) = 0$. For natural transverse (synchrotron) polarization we set $h^\pm = 0$, $\xi^\pm_{x'} = 0$ and $\xi^\pm_{y'} = \pm P$ or, more generally, $\xi^\pm_{x'} = \pm P \sin\Delta$ and $\xi^\pm_{y'} = \pm P\cos\Delta$, implying $X(\varphi) = P^2\cos 2(\varphi-\Delta)$ and $Y(\varphi) = -P^2 \sin 2(\varphi-\Delta)$. The particular combinations $X(\varphi)$ and $Y(\varphi)$ appearing in (A.12) can be written as

$$\begin{aligned} X(\varphi) &= \xi^-_{x_1}\xi^+_{x_1} - \xi^-_{y_1}\xi^+_{y_1}\,, \\ Y(\varphi) &= \xi^-_{x_1}\xi^+_{y_1} + \xi^-_{y_1}\xi^+_{x_1}\,, \end{aligned} \tag{A.13}$$

where now the components $\xi^\pm_{x_1}$, $\xi^\pm_{y_1}$ of the rest-frame polarization vectors refer to the frame Ox₁y₁z' of Fig.2, obtained from the frame Ox'y'z' by the first Euler rotation $R(\varphi, 0, 0)$, i.e.

$$\xi_{x_1} = \xi_{x'}\cos\varphi + \xi_{y'}\sin\varphi\,, \quad \xi_{y_1} = -\xi_{x'}\sin\varphi + \xi_{y'}\cos\varphi\,, \quad \xi_{z_1} = \xi_{z'}\,. \tag{A.14}$$

Thus ξ_{x_1} (ξ_{y_1}) represent the components of $\vec\xi_\perp$ in (normal to) the plane defined by the two axes Oz' and Oz. The meaning of the longitudinal part $\xi_{z'}$ remains unaffected by the rotation $R(\varphi,0,0)$.

Appendix B: The hadron tensors.

Here we consider the hadron tensors appearing in(2.6). In terms of the quantities J_f^μ and A_f^μ introduced in(2.3) we first define the tensors (omitting the flavour index f)

$$H^{\mu\nu}_{JJ} = \overline{J^\mu J^{\nu *}} , \qquad H^{\mu\nu}_{AA} = \overline{A^\mu A^{\nu *}} ,$$

$$H^{\mu\nu}_{JA} = \overline{J^\mu A^{\nu *}} , \qquad H^{\mu\nu}_{AJ} = \overline{A^\mu J^{\nu *}} , \tag{B.1}$$

where the bar means summation over the spins (and eventually other quantum numbers) of the final state particles. We then define in analogy to (A.2) the (hermitian) hadron tensors $H_r^{\mu\nu}$, $r = 1,\dots,4$ by

$$H_1^{\mu\nu} = \frac{1}{2}\left(H^{\mu\nu}_{JJ} + H^{\mu\nu}_{AA} \right),$$

$$H_2^{\mu\nu} = \frac{1}{2}\left(H^{\mu\nu}_{JJ} - H^{\mu\nu}_{AA} \right),$$

$$H_3^{\mu\nu} = \frac{i}{2}\left(H^{\mu\nu}_{JA} - H^{\mu\nu}_{AJ} \right),$$

$$H_4^{\mu\nu} = \frac{1}{2}\left(H^{\mu\nu}_{JA} + H^{\mu\nu}_{AJ} \right). \tag{B.2}$$

For each of these tensors denoted generically by $H^{\mu\nu}$ (omitting the index r) we introduce the following nine independent combinations of its nine space-space- components $H^{mn} = H_{mn}$ $(m,n = 1,2,3)$ or $H_{\rho\sigma} = \epsilon_\rho^m H_{mn} \epsilon_\sigma^{n*}$ $(\rho,\sigma = \pm, 0$, with $\epsilon_+^m = (-1,-i,0)/\sqrt{2}$, $\epsilon_-^m = (1,-i,0)/\sqrt{2}$ and $\epsilon_0^m = (0,0,1)$):

$$\begin{aligned}
\hat{\sigma}_U(H) &= H_{++} + H_{--} &&= H_{11} + H_{22} \\
\hat{\sigma}_L(H) &= H_{00} &&= H_{33} \\
\hat{\sigma}_T(H) &= \mathrm{Re}\, H_{+-} &&= \tfrac{1}{2}(-H_{11} + H_{22}) \\
\hat{\sigma}_4(H) &= \mathrm{Im}\, H_{+-} &&= -\tfrac{1}{2}(H_{12} + H_{21}) = -\mathrm{Re}\, H_{12} , \\
\hat{\sigma}_5(H) &= \tfrac{1}{2}\mathrm{Im}(H_{+0} + H_{-0}) &&= -\tfrac{1}{2\sqrt{2}}(H_{23} + H_{32}) = -\tfrac{1}{\sqrt{2}}\mathrm{Re}\, H_{23} , \\
\hat{\sigma}_6(H) &= \tfrac{1}{2}\mathrm{Re}(H_{+0} - H_{-0}) &&= -\tfrac{1}{2\sqrt{2}}(H_{31} + H_{13}) = -\tfrac{1}{\sqrt{2}}\mathrm{Re}\, H_{31} , \\
\hat{\sigma}_7(H) &= H_{++} - H_{--} &&= -i(H_{12} - H_{21}) = 2\,\mathrm{Im}\, H_{12} , \\
\hat{\sigma}_8(H) &= \tfrac{1}{2}\mathrm{Re}(H_{+0} + H_{-0}) &&= \tfrac{-i}{2\sqrt{2}}(H_{23} - H_{32}) = \tfrac{1}{\sqrt{2}}\mathrm{Im}\, H_{23} , \\
\sigma_9(H) &= \tfrac{1}{2}\mathrm{Im}(H_{+0} - H_{-0}) &&= \tfrac{-i}{2\sqrt{2}}(H_{31} - H_{13}) = \tfrac{1}{\sqrt{2}}\mathrm{Im}\, H_{31} .
\end{aligned} \tag{B.3}$$

We denote this combinations by $\hat{\sigma}_\alpha(H)$, $\alpha = 1,2,\dots,9$ with the special indices U, L, T for $\alpha = 1, 2, 3$. The structure of (B.3) is obvious: decomposing the hermitian tensor H_{mn} into its symmetric (or real) and antisymmetric (or imaginary) part

$$H_{mn} = H_{[m,n]} + H_{\{m,n\}} = \mathrm{Re}\, H_{mn} + i\, \mathrm{Im}\, H_{mn} , \tag{B.4}$$

the six components of $H_{[m,n]} = \mathrm{Re}\, H_{mn}$ contribute only to $\hat{\sigma}_1 \div \hat{\sigma}_6$ (the diagonal elements to $\hat{\sigma}_1 \div \hat{\sigma}_3$, i.e. $\hat{\sigma}_U$, $\hat{\sigma}_L$ and $\hat{\sigma}_T$, the off-diagonal ones to $\hat{\sigma}_4 \div \hat{\sigma}_6$), and the three components of $H_{\{m,n\}} = i\, \mathrm{Im}\, H_{mn}$ only to $\hat{\sigma}_7 \div \hat{\sigma}_9$. Thus a symmetric (antisymmetric) hadron tensor may contribute only to $\hat{\sigma}_1 \div \hat{\sigma}_6$ ($\hat{\sigma}_7 \div \hat{\sigma}_9$).

Table I: Vector and axial-vector couplings of the Z^o to the four groups of fundamental fermions within the Weinberg-Salam model (θ_W is the Weinberg angle)

	v	a
Neutrinos ($Q = 0$) ($\nu_e, \nu_\mu, \nu_\tau, \ldots$)	1	1
Charged leptons ($Q=-1$) ($e^-, \mu^-, \tau^-, \ldots$)	$-1 + 4 \sin^2\theta_W$	-1
Up-quarks ($Q = 2/3$) (u, c, t,...)	$1 - \frac{8}{3} \sin^2\theta_W$	1
Down-quarks ($Q = -1/3$) (d, s, b,...)	$-1 + \frac{4}{3} \sin^2\theta_W$	-1

References

1. S. Weinberg, Phys.Rev.Letters 19, 1264 (1967);
A. Salam, Proc. 8th Nobel Symposium, Stockholm 1968, ed.
N. Swartholm (Almquist and Wiksells, Stockholm, 1968), p.367;
S. Weinberg, Phys. Rev. D5, 1412 (1972)

2. A. DeRujula, R. Petronzio and B. Lautrup, Nucl.Phys. B146, 50 (1978)

3. K. Fabricius, I. Schmitt, G. Kramer and G. Schierholz, DESY Preprint DESY 80/17 (1980), to be published in Phys.Rev.Letters

4. J. Ellis and M. K. Gaillard, CERN Report CERN 76-18 (1976), p.21

5. J. Ellis, Proc. LEP Summer Study, Les Houches and CERN 1978, CERN Report CERN 79-01, Vol.2 (1979), p.615

6. G. Schierholz and D. H. Schiller, DESY Preprint DESY 79/29 (1979), unpublished

7. D. H. Schiller, Z. Physik C3, 21 (1979)

8. E. Laermann, K. H. Streng and P. M. Zerwas, Z. Physik C3, 289 (1980)

8. H. Olsen, P. Osland and I. Overbø, Nucl.Phys. B171, 209 (1980)

9. G. Kramer, G. Schierholz and J. Willrodt, Phys. Letters 78B, 249 (1978), Erratum ibid. 80B, 433 (1979)
G. Schierholz, Proc. SLAC Summer Institute on Particle Physics, Quantum Chromodynamics, 1979, ed. A. Mosher, p.476

10. N. M. Avram and D. H. Schiller, Nucl.Phys. B70, 272 (1974)

11. F. W. Bopp and D. H. Schiller, Z.Physik C, in print

12. K. Koller, D. H. Schiller and D. Wähner, to be published

13. J. D. Bjorken and S. D. Drell, Relativistic Quantum Fields (McGraw-Hill, New York, San Francisco, London, 1965)

Figure Captions

Fig.1 One-photon and one - Z^o exchange diagram for $e^+e^- \to f\bar{f} \to F$.

Fig.2 Definition of Euler angles ϕ, θ and χ. Oz' points into the direction of the electron beam and Ox' into the direction of the Lorentz force. The frame Oxyz is fixed to the final state. Any two noncolinear final state momenta can be chosen to define its relative orientation.

Fig.3 Natural choices of frame Oxyz for three-jet final states. (a) Three-jet event ($T_i = 2E_i/Q$). (b) Helicity frame with Oz along the jet axis (i.e., the axis of the most energetic jet) and Ox pointing into the half-plane of the second most energetic jet. (c) Transversity frame with $O\bar{x}$ along the jet axis and $O\bar{y}$ pointing into the half-plane of the second most energetic jet. Here the quantization axis $O\bar{z}$ is the normal to the event plane.

Fig.4 Azimuthal asymmetry A^f_{21} ($\sim\cos 2\phi$) for leptons and quarks as predicted by the Weinberg-Salam model and $\sin^2\theta_W \approx 0.23$.

Fig.5 Azimuthal asymmetry A^f_{31} ($\sim \sin 2\phi$).

Fig.6 Forward-backward asymmetry A^f_{44} ($\sim \cos\theta$).

Fig.7 Reflection asymmetry ($\theta \to \pi - \theta$, $\chi \to \pi - \chi$) A^f_{14} associated with the imaginary part of the hadronic thesor.

Fig.8 Azimuthal asymmetry A^f_{24} ($\sim \cos 2\phi$) associated with the imaginary part of the hadronic tensor.

Fig.9 Azimuthal asymmetry A^f_{34} ($\sim \sin\phi$) associated with the imaginary part of the hadronic tensor.

Fig.10 Forward-backward asymmetry of the normal to the event plane A^f_{41} ($\sim \cos\bar{\theta}$) associated with the imaginary part of the hadronic tensor.

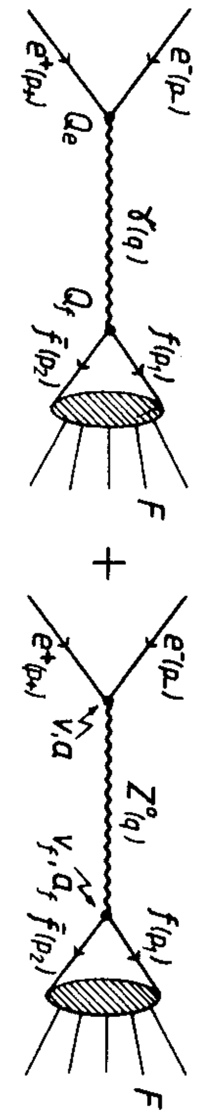

Fig 1

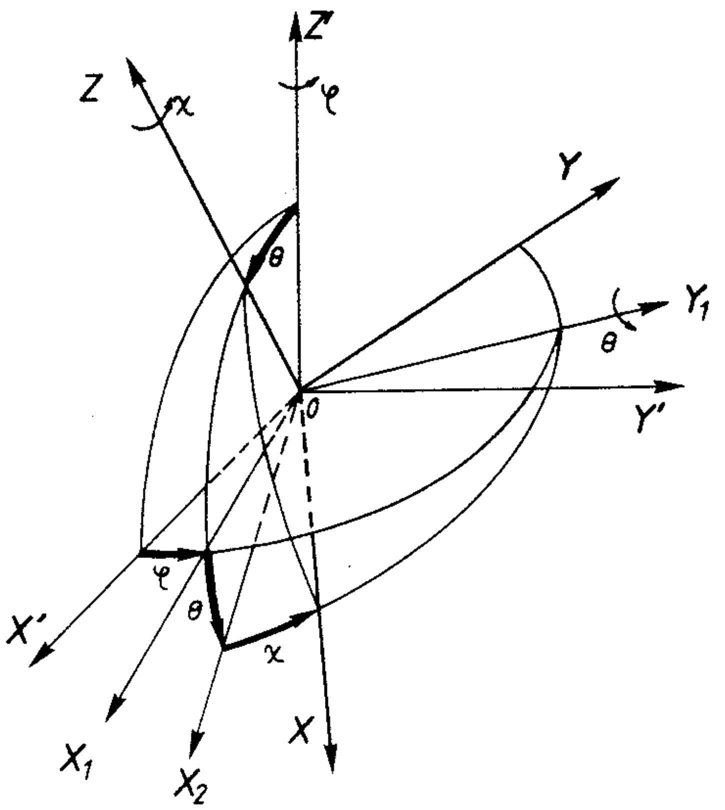

Fig 2

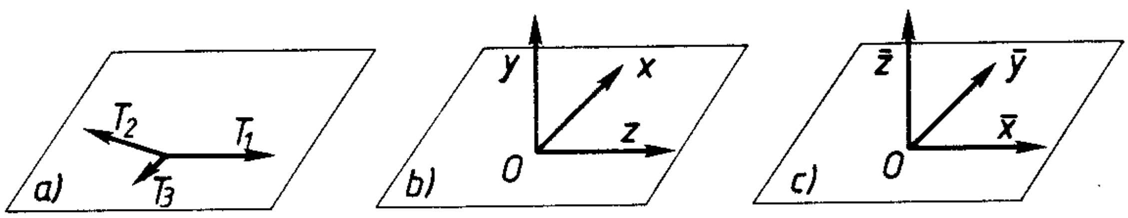

Fig 3

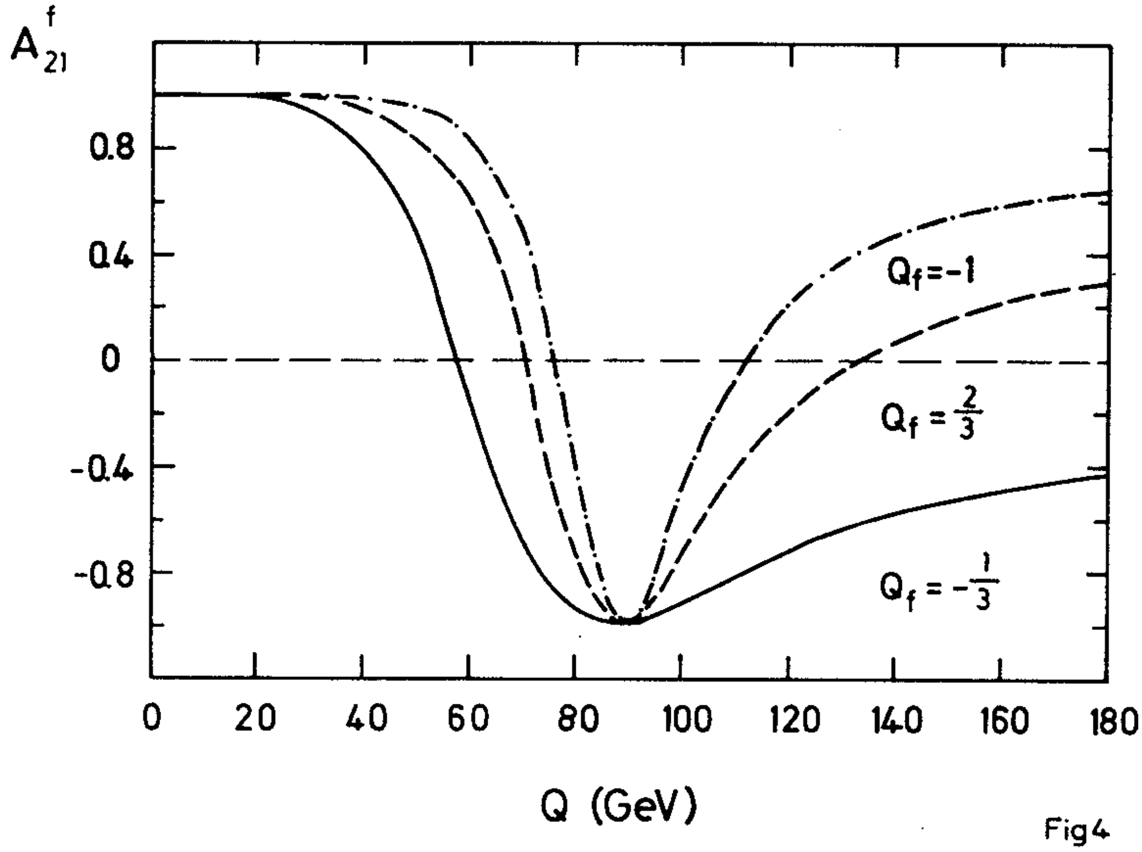

A^f_{21}
0.8
0.4
0
-0.4
-0.8
$Q_f = -1$
$Q_f = \frac{2}{3}$
$Q_f = -\frac{1}{3}$
0
20
40
60
80
100
120
140
160
180
Q (GeV)

Fig4

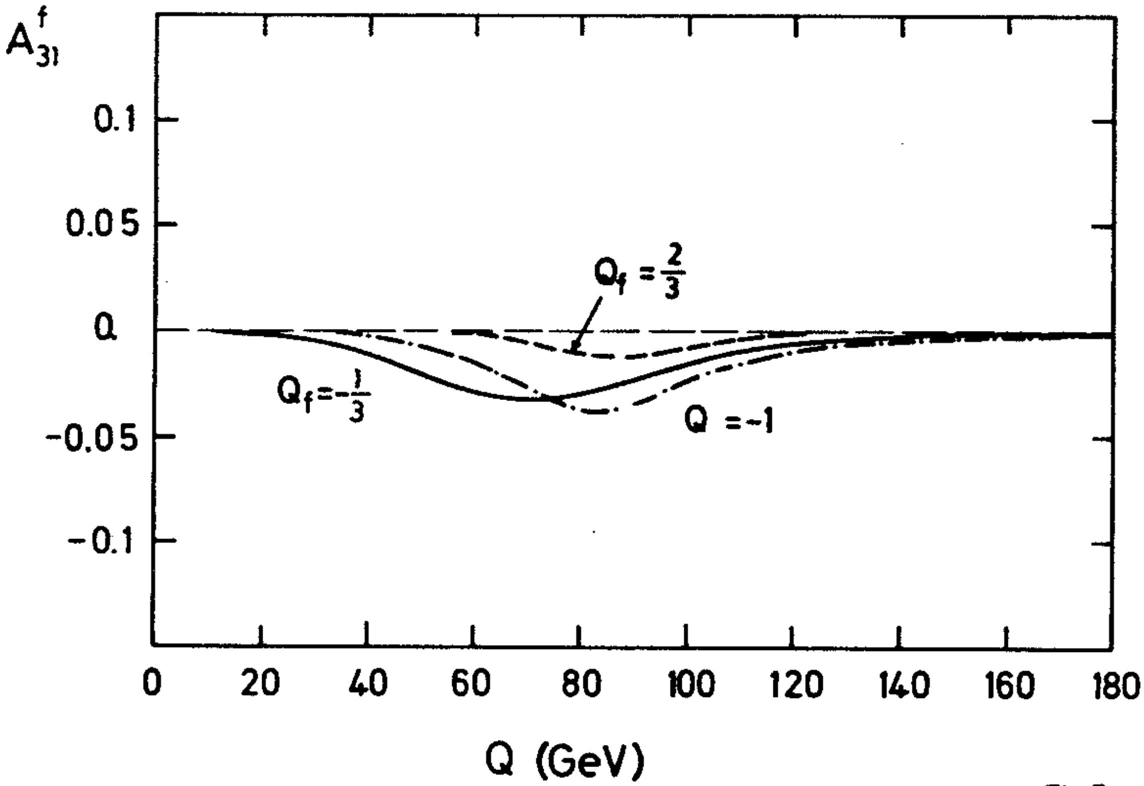

A^f_{31}
0.1
0.05
0
-0.05
-0.1
$Q_f = \frac{2}{3}$
$Q_f = -\frac{1}{3}$
$Q = -1$
0
20
40
60
80
100
120
140
160
180
Q (GeV)

Fig 5

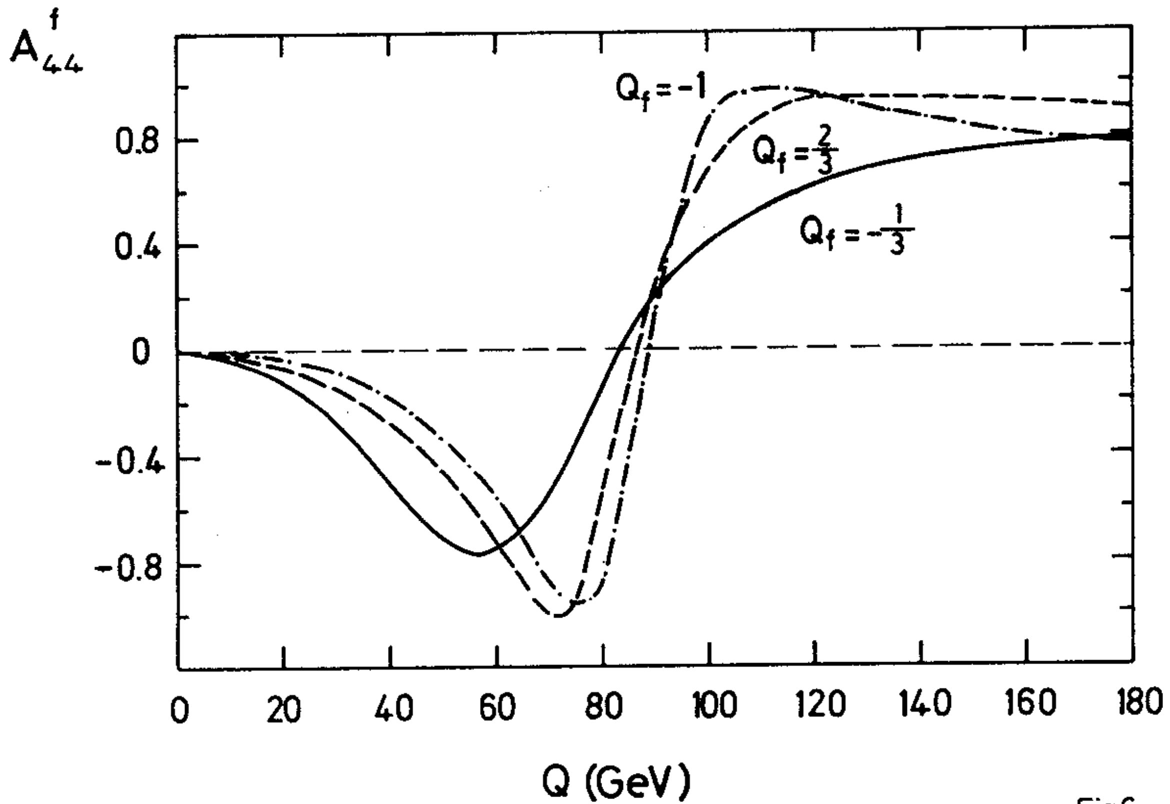

A^f_{44}
0.8
0.4
0
-0.4
-0.8
0
20
40
60
80
100
120
140
160
180
Q (GeV)
$Q_f=-1$
$Q_f=\frac{2}{3}$
$Q_f=-\frac{1}{3}$

Fig 6

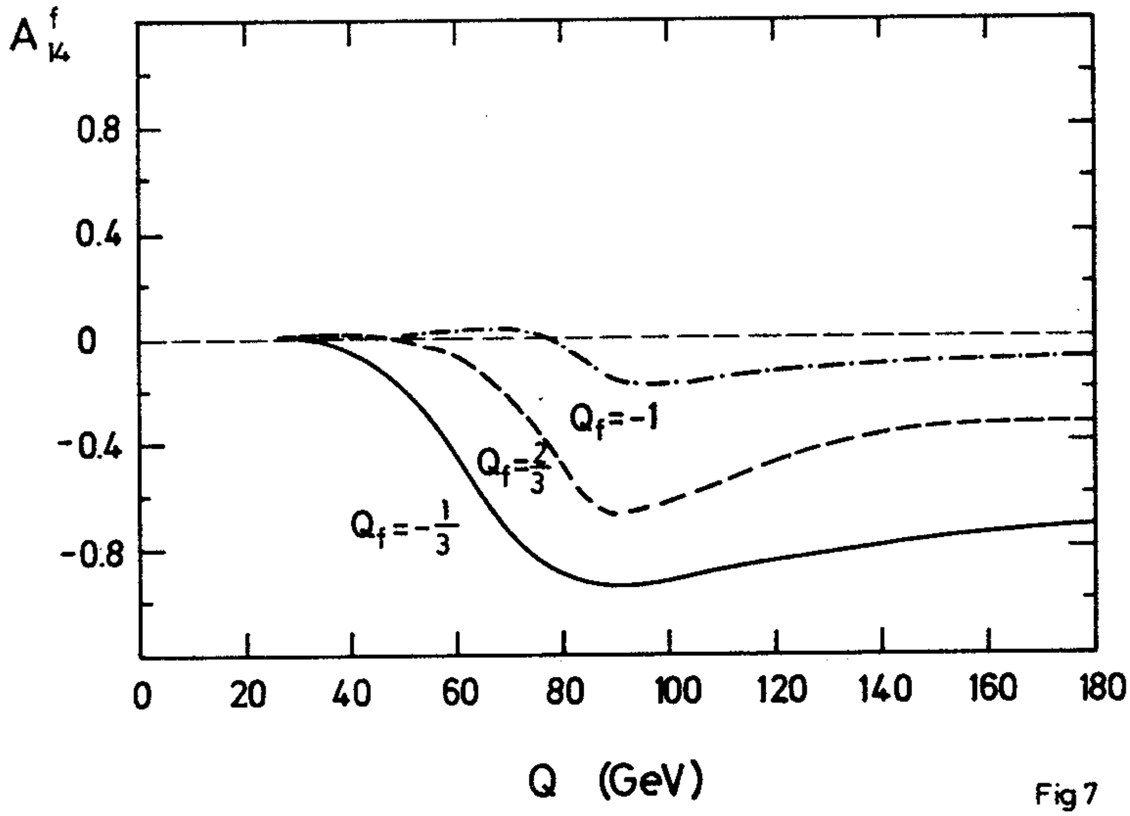

A^f_{14}
0.8
0.4
0
-0.4
-0.8
0
20
40
60
80
100
120
140
160
180
Q (GeV)
$Q_f=-1$
$Q_f=\frac{2}{3}$
$Q_f=-\frac{1}{3}$

Fig 7

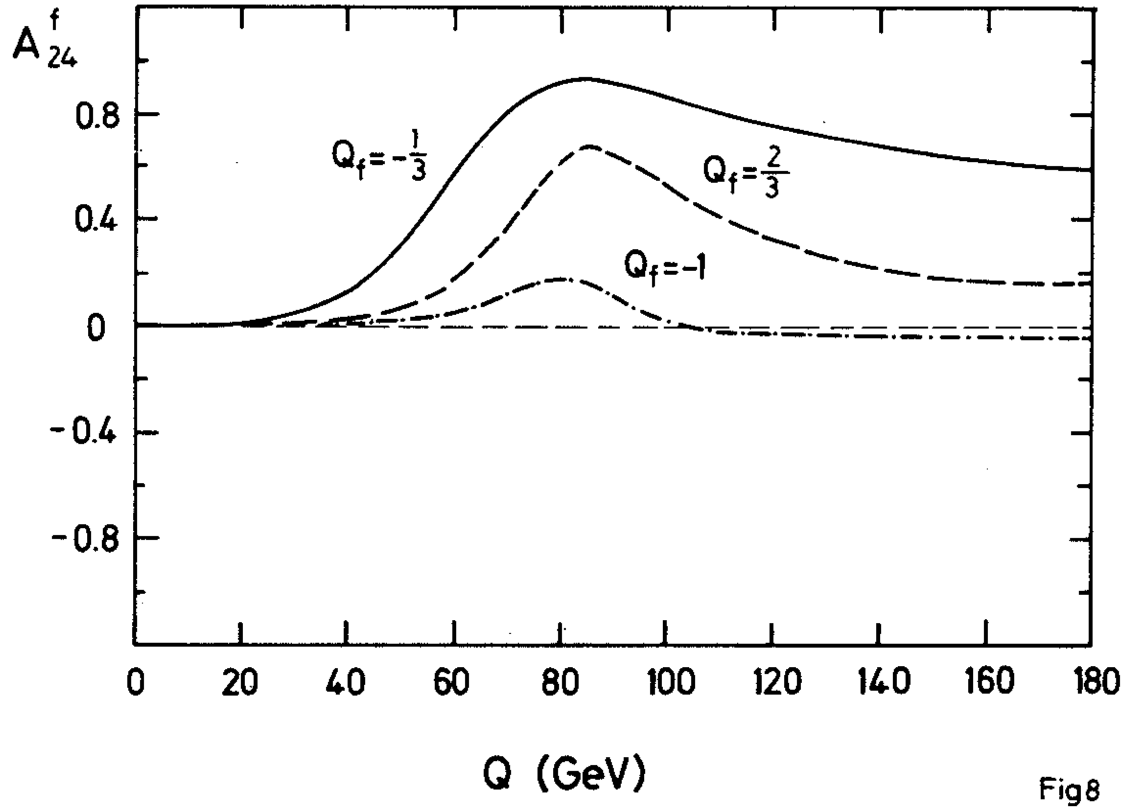

A^f_{24}
0.8
0.4
0
-0.4
-0.8
$Q_f=-\frac{1}{3}$
$Q_f=\frac{2}{3}$
$Q_f=-1$
0
20
40
60
80
100
120
140
160
180
Q (GeV)

Fig 8

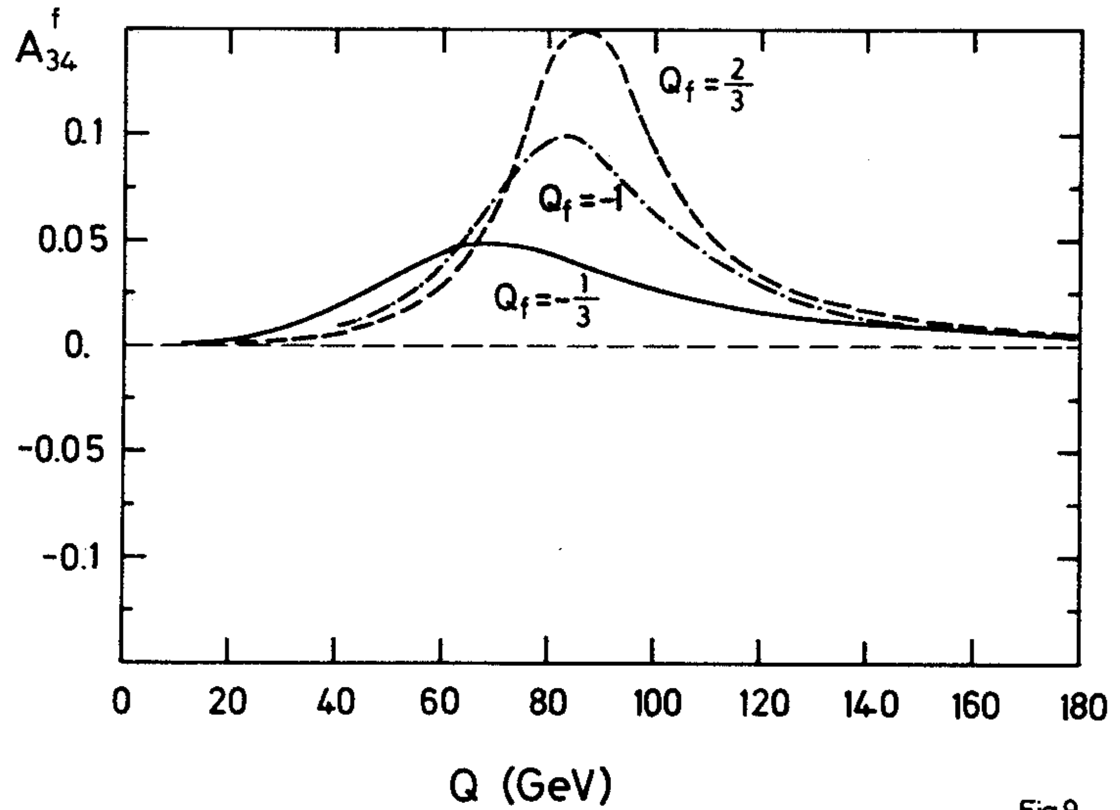

A^f_{34}
0.1
0.05
0.
-0.05
-0.1
$Q_f=\frac{2}{3}$
$Q_f=-1$
$Q_f=-\frac{1}{3}$
0
20
40
60
80
100
120
140
160
180
Q (GeV)

Fig 9

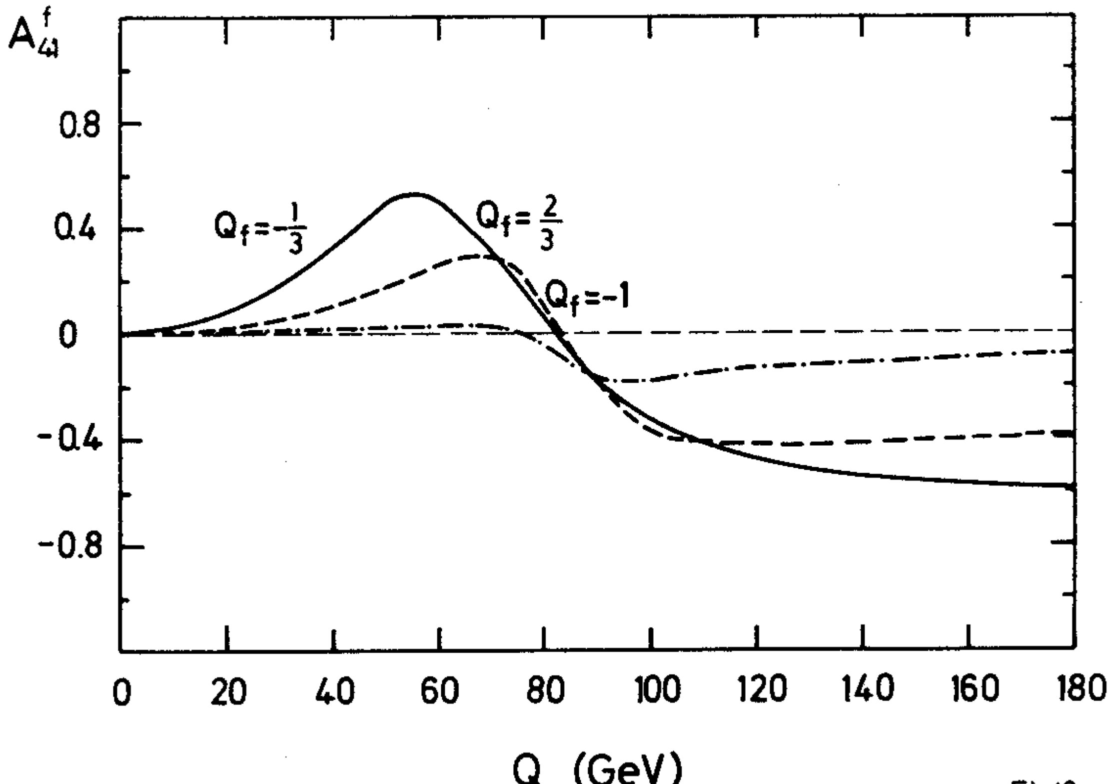

A_{41}^{f}
0.8
0.4
0
-0.4
-0.8
$Q_f=-\frac{1}{3}$
$Q_f=\frac{2}{3}$
$Q_f=-1$
0
20
40
60
80
100
120
140
160
180
Q (GeV)

Fig10